iScience

CellPress
OPEN ACCESS

Article

Notch activation defines immune-suppressive subsets of ccRCCs with unfavorable benefits from immunotherapy over VEGFR/mTOR inhibitors

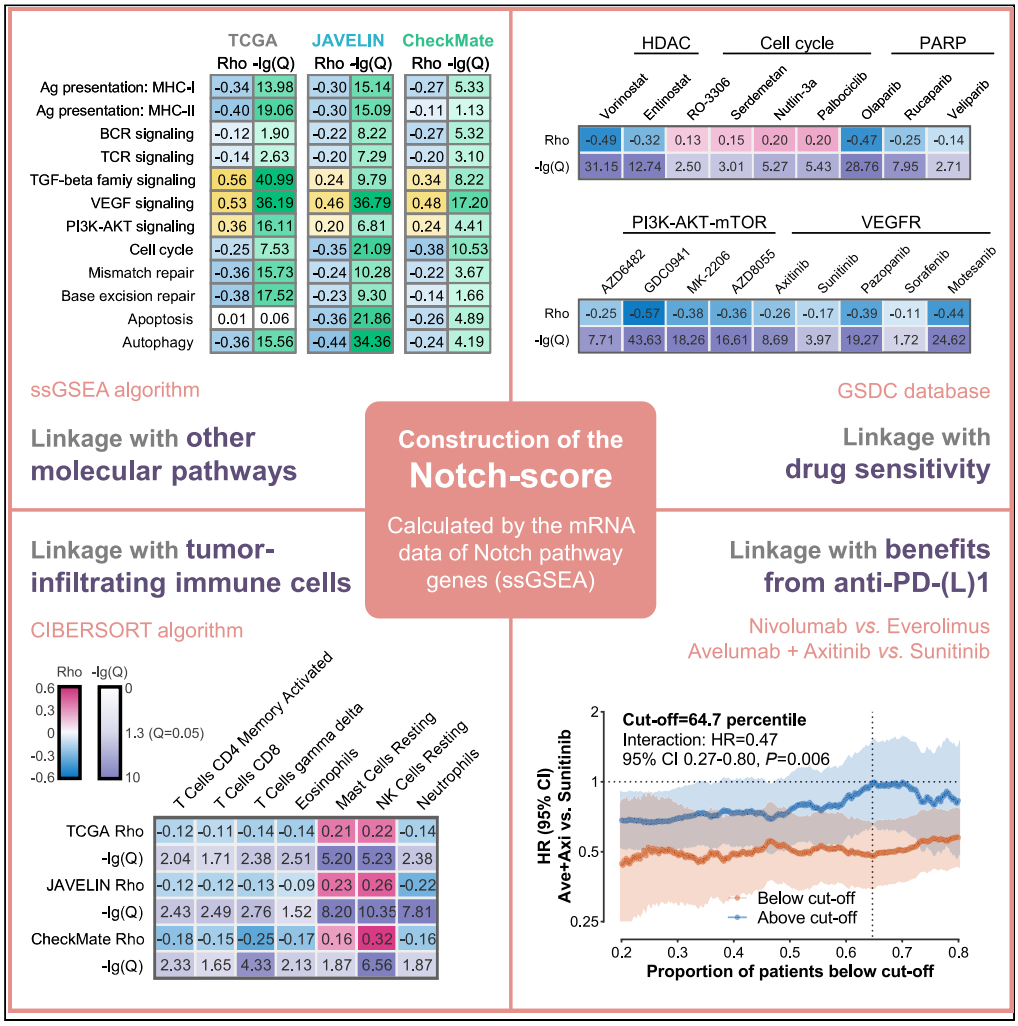

Sujun Han, Yu Xu, Dong Chen, ..., Wenxian Wang, Shangli Cai, Nianzeng Xing

xingnz@cicams.ac.cn

Highlights

The Notch-score was built using mRNA expression of Notch pathway genes

The score was linked with Notch activation, angiogenesis, and mTOR activity

A high score defined an immune-suppressive subset of ccRCCs

A high score indicated poor benefits from immunotherapy over VEGFR/mTOR inhibitors

Han et al., iScience 27, 108290
January 19, 2024 © 2023
https://doi.org/10.1016/j.isci.2023.108290

iScience

CellPress
OPEN ACCESS

Article

Notch activation defines immune-suppressive subsets of ccRCCs with unfavorable benefits from immunotherapy over VEGFR/mTOR inhibitors

Sujun Han,[1,7] Yu Xu,[2,7] Dong Chen,[1] Feiya Yang,[1] Mingshuai Wang,[1] Qiaoxia Zhou,[2] Guoqiang Wang,[2] Leo Li,[2] Chunwei Xu,[3] Wenxian Wang,[4] Shangli Cai,[2] and Nianzeng Xing[1,5,6,8,*]

SUMMARY

The evolutionarily conserved Notch pathway, involved in cancer stem cell capacity and cancer immunity, may predict the benefit from immune checkpoint inhibitors (ICIs) in clear cell renal cell carcinoma (ccRCC). In the TCGA dataset, mRNA expression of Notch pathway genes identified three clusters with different prognoses and molecular characteristics. Based on the differentially expressed Notch pathway genes between clusters, we constructed the Notch-score, correlated with Notch activation, angiogenesis, PI3K-AKT-mTOR activity, and sensitivities to VEGFR/mTOR inhibitors. A high Notch-score was linked with more "resting"/"anti-inflammatory" rather than "activated"/"pro-inflammatory" tumor-infiltrating immune cells, inactivated immune pathways, and scarce any benefits from ICI-based therapies over VEGFR/mTOR inhibitors in the JAVELIN Renal 101 (avelumab plus axitinib vs. sunitinib) and the CheckMate-009/010/025 trials (nivolumab vs. everolimus). For the Notch-activated ccRCCs, ICIs provide limited advantages and might not be strongly recommended, by which the cost-effectiveness of treatments in ccRCCs may be potentially improved.

INTRODUCTION

Worldwide, renal cell carcinoma (RCC) strikes more than 400,000 people annually,[1] of which approximately 70% are the clear cell RCC (ccRCC) subtype.[2] For early-stage ccRCCs, surgical or ablative strategies can be effective; however, nearly one-third of patients present with advanced diseases develop metastasis.[3] Due to the chemotherapy-resistant feature of ccRCCs, the prognosis of late-stage patients was dismal until targeted agents and immune checkpoint inhibitors (ICIs) became integrated into treatment algorithms.[4] Compared to targeted therapies, ICI-based immunotherapies deliver the opportunity for a long-term response, although observed merely in a minority of patients.[5–7] These phenomena emphasize the vitality of investigating biomarkers linked with the benefits from ICI-based immunotherapies over conventional inhibitors targeting mTOR or vascular endothelial growth factor receptor (VEGFR), which might provide guidance for individualized treatment choice and management of ccRCCs.

The Notch pathway is an evolutionarily highly conserved signaling mechanism that occurs via short-range cell-cell interaction between Notch receptors (NOTCH1-4) and ligands (Jagged1, Jagged2, delta-like canonical NOTCH ligand 1 [DLL1], DLL3, and DLL4).[8] Receptor-ligand interaction leads to proteolytic cleavage of the receptor by ADAM metalloproteases and γ-secretases,[9] liberating the intracellular domain of Notch receptor (NICD). The NICD then migrates to the nucleus, where it regulates cell fate determination, differentiation, and tissue-specific gene expression.[9,10] In addition, the NICD can participate in a variety of non-canonical signals, such as nuclear factor-κB, PI3K-AKT, WNT, and transforming growth factor β (TGF-β).[11]

The Notch signaling plays crucial roles in kidney development, maintenance, and disease. In the developing kidney, the Notch signaling regulates the maturation/exit of nephron progenitor cells, nephron formation and segmentation, proximal tubule morphogenesis, the "salt and pepper" patterning of principal and intercalated cells in collecting duct, and ureteric bud branching.[12] In the developed kidney, this

[1]Department of Urology, National Cancer Center/National Clinical Research Center for Cancer/Cancer Hospital, Chinese Academy of Medical Sciences and Peking Union Medical College, Beijing, China
[2]Burning Rock Biotech, Guangzhou, Guangdong, China
[3]Institute of Basic Medicine and Cancer (IBMC), Chinese Academy of Sciences, Hangzhou, Zhejiang, China
[4]Department of Clinical Trial, The Cancer Hospital of the University of Chinese Academy of Sciences (Zhejiang Cancer Hospital), Hangzhou, Zhejiang, China
[5]State Key Laboratory of Molecular Oncology, National Cancer Center/National Clinical Research Center for Cancer/Cancer Hospital, Chinese Academy of Medical Sciences and Peking Union Medical College, Beijing, China
[6]Department of Urology, Shanxi Province Cancer Hospital/Shanxi Hospital Affiliated to Cancer Hospital, Chinese Academy of Medical Sciences/Cancer Hospital Affiliated to Shanxi Medical University, Taiyuan, Shanxi, China
[7]These authors contributed equally
[8]Lead contact
*Correspondence: xingnz@cicams.ac.cn
https://doi.org/10.1016/j.isci.2023.108290

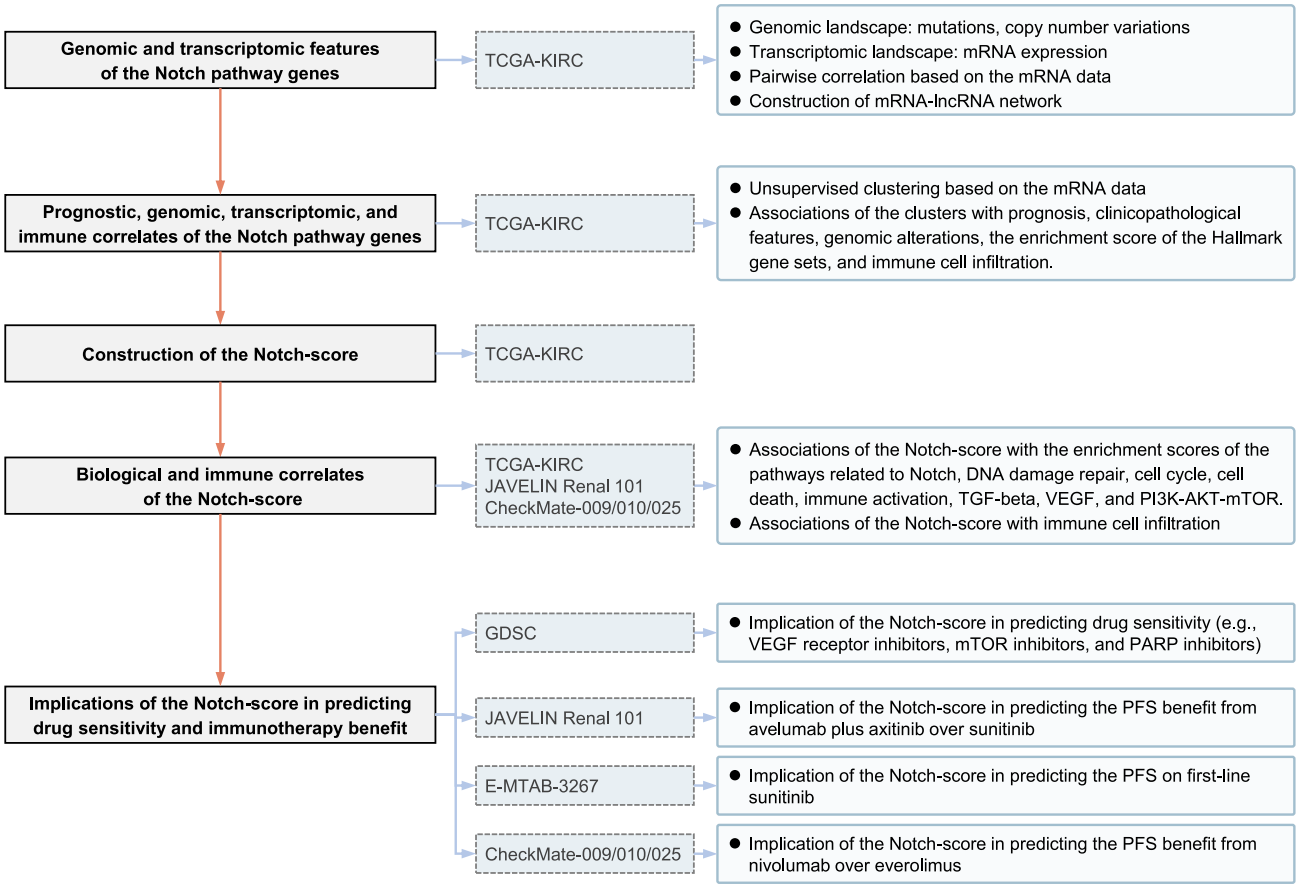

Figure 1. Study design

Abbreviations: PARP = poly-ADP-ribose polymerase, TCGA-KIRC = The Cancer Genome Atlas-Kidney Renal Clear Cell Carcinoma. TGF = transforming growth factor, VEGF = vascular endothelial growth factor.

signaling also controls the ratio of principal cells to intercalated cells in collecting duct and is engaged in the pathogenesis of acute/chronic renal injury, diabetic nephropathy, hereditary diseases such as Alagille syndrome and Hajdu-Cheney syndrome, and kidney cancers.[12–17]

The Notch pathway is involved in many aspects of cancer biology and antitumor immunity. First, the Notch signaling regulates the self-renewal and differentiation of cancer stem cells (CSCs).[18] CSCs can promote immune escape by regulating tumor-associated macrophages which in turn affected the differentiation and proliferation of CSCs through cytokines.[19] Second, the Notch pathway mediates the communication between tumor cells and tumor immune microenvironment (TIME). In basal-like triple-negative breast cancer, a Notch-dependent paracrine loop between tumor cells and macrophages leads to suppressive TIME.[20] Anti-Jagged1/2 therapy in tumor-bearing mouse models enhanced the efficacy of T cell-based immunotherapy, partly via increasing the infiltration levels of reactive $CD8^+$ T cells and $CD11c^+$ immunostimulatory cells.[21] Third, in ccRCC, the Notch signaling can positively regulate angiogenesis via the DLL4-NOTCH and the Jagged1-NOTCH bindings,[22] and angiogenesis was negatively linked with inflamed TIME and immunotherapy benefit.[23–26]

Based on these observations indicating the pivotal roles of Notch activation in regulating CSC maintenance, angiogenesis, DDR, and TIME, we hypothesized that Notch activation might define an immune-suppressive phenotype associated with the poor benefit from ICIs in ccRCC. In this study, we aimed to (i) describe the genomic and transcriptomic features of the Notch pathway genes, (ii) construct the Notch-score reflecting Notch activation, (iii) explore the biological and immune correlates of the Notch-score, and (iv) investigate the associations of the Notch-score with drug sensitivities (e.g., VEGFR/mTOR inhibitors) and the benefit from ICI-based immunotherapy over VEGFR/mTOR inhibitors in advanced ccRCCs (summarized in Figure 1).

RESULTS

The genomic and transcriptomic landscapes of the Notch pathway genes

Based on the Notch pathway-related signatures in the cBioPortal platform and molecular signatures database and previous researches,[15,27,28] 62 genes (4 Notch receptors, 30 related to transmitting signal to the nucleus, and 28 related to the transcriptional regulation by the NICD, Table S1) were determined as the Notch pathway genes and were analyzed in our study.

In The Cancer Genome Atlas-Kidney Renal Clear Cell Carcinoma (TCGA-KIRC) cohort, the frequencies of genomic alterations of most Notch pathway genes were low (<5.0%), except *MAML1* (25.3%), *KAT2B* (13.6%), *SPEN* (12.3%), and *EP300* (6.3%, Figure S1). Particularly, deep deletions were enriched in *KAT2B* and amplifications were common in *MAML1*. These results are similar to those in a previous study analyzing an older version of the TCGA cohort with a different analytical pipeline.[29]

Mutations of any Notch pathway gene (referred to as "Notch mutations" hereafter) were observed in 72.9% of samples. Notch mutations co-occurred with the mutations in *VHL* (odd's ratio [OR] = 1.68, p = 0.015), *PBRM1* (OR = 1.97, p = 0.002), *SETD2* (OR = 2.20, p = 0.004), *ARID1A* (OR = 3.77, p = 0.002), *BAP1* (OR = 2.72, p = 0.001), *PTEN* (OR = 3.54, p = 0.057), and *TP53* (OR = 3.76, p = 0.044), and Notch mutations and *KDM5C* mutations tended to be mutually excluded (OR = 0.52, p = 0.084). Compared to normal renal tissues, 66.1% (41/62) of the Notch pathway genes expressed higher and 14.5% (9/62) expressed lower in the tumor samples (Figure 2A). Taken together, the genomic and transcriptomic alterations of the Notch pathway genes indicate their potential roles in the tumorigenesis and development of ccRCC.

The Notch pathway defines an aggressive subtype with immune suppression

We first analyzed the pairwise correlations between the mRNA level of each Notch pathway gene (Figure 2B). Most expression levels were positively correlated with each other, except for *RBPJL*, *PSENEN*, *DLL3*, and *HES7*. Moreover, we performed unsupervised clustering based on the mRNA levels of the 62 Notch pathway genes. According to the curve of cost change of K-medoids (Figure S2), classifying all ccRCC samples into 3 clusters was optimal (Figure 2C). The mRNA expression of these genes in the mRNA-cluster B was between the mRNA-clusters A and C (Table S2), indicating that the mRNA-cluster B does not represent a unique subtype, but rather an intermediate state between the mRNA-clusters A and C.

Most genes tended to express higher in the mRNA-cluster A except *RBPJL*, *PSENEN*, *DLL3*, and *HES7* (Table S2), consistent with the result of pairwise correlation. Moreover, the mRNA-cluster A with higher expression of most genes had a better prognosis, while the mRNA-cluster C with relatively lower expression had a poorer overall survival (OS, $p < 0.001$, Figure 2D), consistent with previous results suggesting the relationship between long survival and high expression of *NOTCH1*, *JAG1/2*, *DLL4*, and *HEY1*.[30] We further analyzed the pairwise correlation between each long non-coding RNA (lncRNA) and the mRNA expression of each Notch pathway gene (Figure S3A). The mRNA-lncRNA pairs with a correlation R value over 0.80 and a p value below 0.05 were selected for constructing the mRNA-lncRNA network (Figure S3B). These lncRNAs might possess potentials of regulating the expression of corresponding Notch pathway genes.

Furthermore, we estimated the associations of the mRNA-cluster with (i) clinicopathological features, (ii) the genomic alterations of commonly mutated genes, (iii) the enrichment score of HALLMARK gene sets, and (iv) immune cell infiltration. The mRNA-cluster C tended to have less mutations in *VHL* (39.5% vs. 54.8%, p = 0.046) and *PBRM1* (37.0% vs. 51.6%, p = 0.087, Figure 3A). The mRNA-cluster A with higher expression of most Notch pathway genes had higher scores of the pathways related to Notch ($p < 0.001$), angiogenesis ($p < 0.001$), and PI3K-AKT-mTOR ($p < 0.001$, Figure 3B), suggesting that the activation of Notch pathway might be associated with a better response to antiangiogenic agents and PI3K-AKT-mTOR inhibitors. In addition, the mRNA-cluster C had a higher score of the DNA damage repair pathway ($p < 0.001$) and a lower score of the TGF-β pathway ($p < 0.001$, Figure 3B) and tended to have more "activated"/"pro-inflammatory" rather than "resting"/"anti-inflammatory" tumor-infiltrating immune cells (TIICs, Figure 3C). For instance, fewer resting memory $CD4^+$ T cells ($p < 0.001$), resting natural killer (NK) cells (p = 0.086), and resting mast cells ($p < 0.001$), and more activated memory $CD4^+$ T cells (p = 0.023), activated NK cells (p = 0.021), $CD8^+$ T cells (p = 0.011), and follicular helper T cells ($p < 0.001$) were observed in the mRNA-cluster C. The inactivation of the TGF-β pathway and the activation of immune cells have been shown to promote tumor response to ICI treatment.[31] Taken together, these results suggest that the Notch inactivation might indicate a poor response to VEGFR/mTOR inhibitors and a favorable response to ICI treatment in ccRCC.

Construction of a Notch-score and its biological and immune correlates

We aimed to establish a score to estimate the level of Notch activation for the following biomarker analysis (referred to as the Notch-score). The mRNA-cluster B was intermediate between the mRNA-clusters A and C, in terms of expression of Notch pathway genes (Figure 2C and Table S2), survival (Figure 2D), ssGSEA scores of HALLMARK pathways (Figure 3B), and immune cell infiltration (Figure 3C). Given these, by using the differentially expressed genes between the mRNA-clusters A and C, we could establish a score to reflect Notch activation.

We compared the mRNA expression of Notch pathway genes between the mRNA-cluster A and C. In total, 55 Notch pathway genes were highly expressed in the mRNA-cluster A, and two were lowly expressed (adjusted p value < 0.05, Figure 4A and Table S2). The 2 "lowly expressed" genes are *DLL3* and *PSENEN*. DLL3 has been identified as an inhibitory Notch ligand,[15] and the knockdown of *PSENEN* by siRNA upregulated the expression of *NOTCH1* in adipocytes.[32] We also observed negative correlations between the mRNA levels of *PSENEN* and NOTCH receptor genes (*NOTCH1-4*, Figure 4A). These results suggest that the expression of *DLL3* and *PSENEN* might be negatively correlated with Notch activation.

To reflect the level of Notch activation in ccRCCs, we constructed the Notch-score using the 55 "highly expressed" and 2 "lowly expressed" Notch pathway genes. First, we separately calculated the two ssGSEA scores of the "highly expressed" and the "lowly expressed" genes. Then, the value of the ssGSEA score for "highly expressed" genes minus the score for "lowly expressed" genes was defined as the Notch-score (Figure 4A), which could effectively differentiate the samples of the mRNA-clusters A, B, and C ($p < 0.001$). The Notch-score was lower in the samples with worse histological grade ($p < 0.001$), or in the TCGA-4 cluster in the TCGA Research Network study[33] ($p < 0.001$, Figure 4B). Besides, the Notch-score was not associated with sex ($p > 0.10$) and TNM stage ($p > 0.10$, Figure 4B).

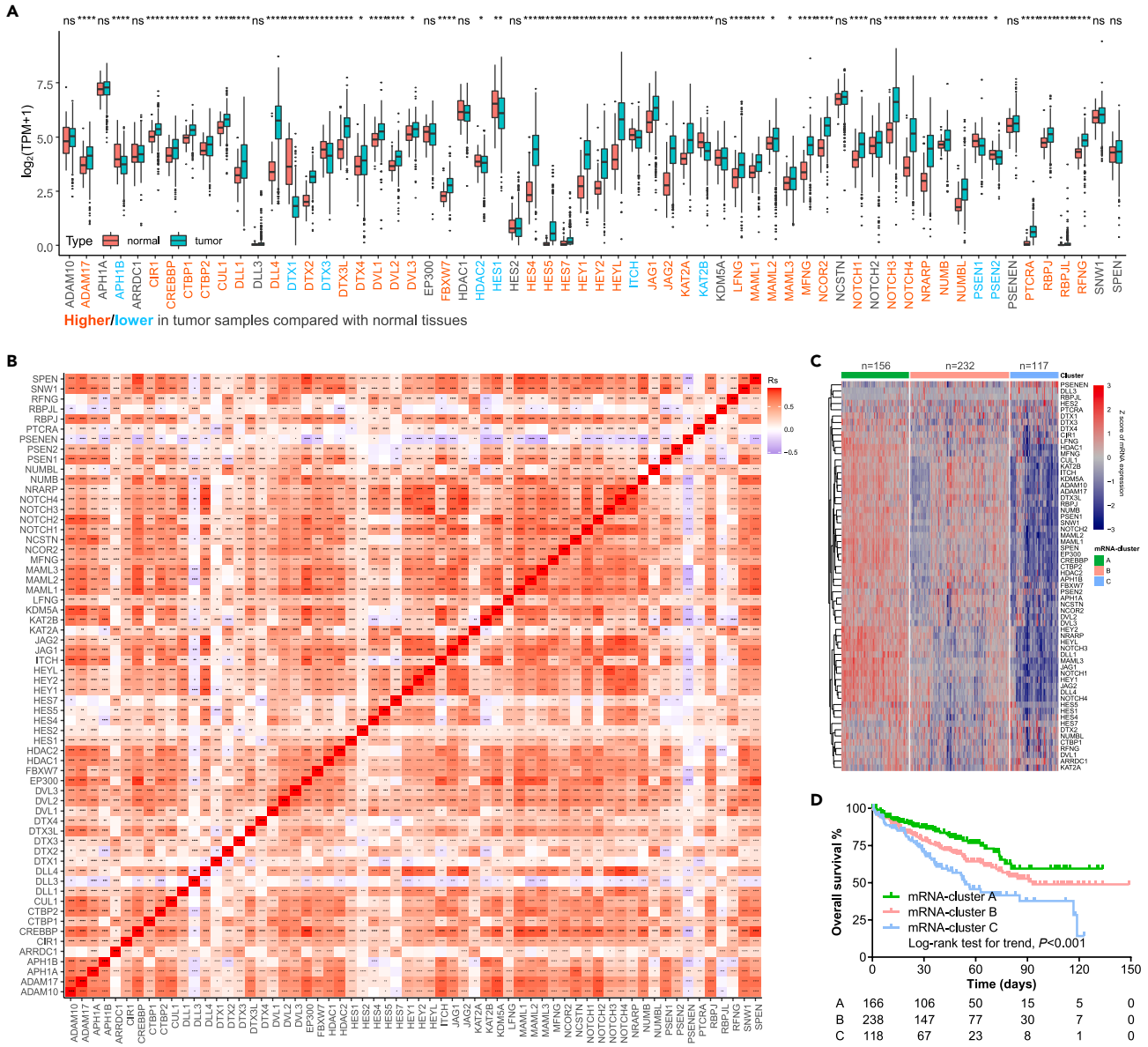

Figure 2. Clustering based on the expression of the Notch pathway genes

(A) The mRNA expression of the Notch pathway genes and the tumor and normal kidney tissues in the TCGA-KIRC cohort. Data are displayed as median and quartiles. The Mann-Whitney test: *, $p < 0.05$; **, $p < 0.01$; ***, $p < 0.001$.

(B) Pairwise correlation of the Notch pathway genes in the TCGA-KIRC cohort.

(C) Unsupervised clustering based on the mRNA expression of the Notch pathway genes in the TCGA-KIRC cohort.

(D) Association of the mRNA-clusters with overall survival in the TCGA-KIRC cohort. Abbreviations: TCGA-KIRC = The Cancer Genome Atlas-Kidney Renal Clear Cell Carcinoma.

To evaluate the robustness of the Notch-score, we analyzed a wider range of signatures (1,603 Reactome signatures) in the three independent cohorts including the TCGA-KIRC dataset, the JAVELIN Renal 101 trial (abbreviated as "JAVELIN" hereinafter), and the CheckMate-009/010/025 (CM-009/010/025) trials. To begin with, we calculated Spearman's correlations of the Notch-score with the ssGSEA scores of the 1,603 Reactome signatures in these three cohorts (Figure 4C; for detailed results, please see Data S1). Although the TCGA dataset is dominated by early-stage ccRCCs while the other two trials include advanced/metastatic ccRCCs only, these correlations of the Notch-score with other pathways in different cohorts were highly consistent (TCGA and JAVELIN: Rho = 0.82, $p < 0.001$; TCGA and CM: Rho = 0.77, $p < 0.001$; JAVELIN and CM: Rho = 0.87, $p < 0.001$, Figure 4D), demonstrating the considerable credibility of the Notch-score in both early- and late-stage ccRCCs.


A
mRNA-cluster
Mutation count
Fraction genome altered
Age
Sex
TNM stage
Grade
Notch mutations
VHL
PBRM1
SETD2
ARID1A
SMARCA4
BAP1
KDM5C
PTEN
MTOR
PIK3CA
TP53
mRNA-cluster
A
B
C
Sex
female
male
Mutation count
TNM stage
I
II
III
IV
Fraction genome altered
Grade
G1
G2
G3
G4
Age
<65
>65
Notch mutations
No
Yes
B
mRNA-cluster
HALLMARK_MITOTIC_SPINDLE
HALLMARK_E2F_TARGETS
HALLMARK_G2M_CHECKPOINT
HALLMARK_MYC_TARGETS_V1
HALLMARK_UNFOLDED_PROTEIN_RESPONSE
HALLMARK_MTORC1_SIGNALING
HALLMARK_MYC_TARGETS_V2
HALLMARK_DNA_REPAIR
HALLMARK_SPERMATOGENESIS
HALLMARK_HEME_METABOLISM
HALLMARK_PANCREAS_BETA_CELLS
HALLMARK_COAGULATION
HALLMARK_XENOBIOTIC_METABOLISM
HALLMARK_UV_RESPONSE_UP
HALLMARK_CHOLESTEROL_HOMEOSTASIS
HALLMARK_REACTIVE_OXYGEN_SPECIES_PATHWAY
HALLMARK_MYOGENESIS
HALLMARK_APICAL_JUNCTION
HALLMARK_KRAS_SIGNALING_DN
HALLMARK_ESTROGEN_RESPONSE_EARLY
HALLMARK_ESTROGEN_RESPONSE_LATE
HALLMARK_APICAL_SURFACE
HALLMARK_ANGIOGENESIS
HALLMARK_EPITHELIAL_MESENCHYMAL_TRANSITION
HALLMARK_HEDGEHOG_SIGNALING
HALLMARK_NOTCH_SIGNALING
HALLMARK_WNT_BETA_CATENIN_SIGNALING
HALLMARK_TGF_BETA_SIGNALING
HALLMARK_UV_RESPONSE_DN
HALLMARK_ALLOGRAFT_REJECTION
HALLMARK_IL6_JAK_STAT3_SIGNALING
HALLMARK_INTERFERON_GAMMA_RESPONSE
HALLMARK_INTERFERON_ALPHA_RESPONSE
HALLMARK_HYPOXIA
HALLMARK_GLYCOLYSIS
HALLMARK_P53_PATHWAY
HALLMARK_TNFA_SIGNALING_VIA_NFKB
HALLMARK_KRAS_SIGNALING_UP
HALLMARK_APOPTOSIS
HALLMARK_COMPLEMENT
HALLMARK_INFLAMMATORY_RESPONSE
HALLMARK_IL2_STAT5_SIGNALING
HALLMARK_PI3K_AKT_MTOR_SIGNALING
HALLMARK_ANDROGEN_RESPONSE
HALLMARK_PROTEIN_SECRETION
HALLMARK_FATTY_ACID_METABOLISM
HALLMARK_ADIPOGENESIS
HALLMARK_BILE_ACID_METABOLISM
HALLMARK_PEROXISOME
HALLMARK_OXIDATIVE_PHOSPHORYLATION
mRNA-cluster
A
B
C
Enrichment Score
Q value
ns
* <0.05
** <0.01
*** <0.001
**** <0.0001
C
CIBERSORT (relative proportion)
mRNA-cluster A
mRNA-cluster B
mRNA-cluster C
B Cells Memory
B Cells Naive
Dendritic Cells Activated
Dendritic Cells Resting
Eosinophils
Macrophages M0
Macrophages M1
Macrophages M2
Mast Cells Activated
Mast Cells Resting
Monocytes
Neutrophils
NK Cells Activated
NK Cells Resting
Plasma Cells
T Cells CD4 Memory Activated
T Cells CD4 Memory Resting
T Cells CD4 Naive
T Cells CD8
T Cells Follicular Helper
T Cells gamma delta
T Cells Regulatory Tregs

Figure 3. Associations of the mRNA-clusters with clinicopathological features, genomic alterations, hallmark pathways, and immune cell infiltration

(A–C) The associations of the mRNA-clusters with clinicopathological features and the genomic alterations of commonly mutated genes (A), the enrichment score of Hallmark gene sets (B), and immune cell infiltration (C) in the TCGA-KIRC cohort. Data are displayed as median and quartiles. The Kruskal-Wallis test: *, Q < 0.05; **, Q < 0.01; ***, Q < 0.001. Abbreviations: TCGA-KIRC = The Cancer Genome Atlas-Kidney Renal Clear Cell Carcinoma.

First, the Notch-score was remarkably associated with the enrichment scores related to the Notch pathway (Figure 4E), indicating that the Notch-score can reflect the level of Notch activation. Second, the Notch-score was negatively correlated with the scores related to DNA repair, cell cycle, cell death, antigen processing and presentation, B/T cell receptor downstream signaling, and metabolism of steroids, and was positively correlated with the scores concerning the TGF-β, PI3K-AKT, and VEGF pathways (Figure 4E). Third, consistent with the previously described results, the Notch-score tended to be correlated with more "resting"/"anti-inflammatory" rather than "activated"/"pro-inflammatory" TIICs (Figure 4F). Taken together, these results indicate the robust associations of the Notch-score with pathway activity and TIME, and might suggest the potential utility of the Notch-score in predicting the responses to VEGFR/mTOR inhibitors and immunotherapy in ccRCC.

Associations of the Notch-score with drug sensitivity in ccRCC cell lines

Based on the IC_{50} data of ccRCC cell lines in the Genomics of Drug Sensitivity in Cancer database, we analyzed the associations of the Notch-score with the sensitivities to targeted agents (Figure 4G). Histone deacetylase (HDAC) inhibitors induce growth arrest and apoptosis via modulating multiple pathways in cancer cell lines; however, these inhibitors can also lead to Notch activation that partially attenuates their antitumor activities in return.[34,35] This side effect was speculated to be redundant in the tumor cells where the Notch signaling has already been strongly activated. This hypothesis was supported, to some extent, by the association between a high Notch-score and sensitivities to HDAC inhibitors, such as vorinostat (Q < 0.001) and entinostat (Q < 0.001, Figure 4G).

Poly-ADP-ribose polymerase (PARP) inhibitors exert antitumor functions in the tumors with homologous recombination deficiency. In accordance with the negative correlation between the Notch-score and the activation of homologous recombination repair (Figure 4E), the Notch-score was negatively associated with the IC_{50} of PARP inhibitors (Figure 4G). In addition, a high Notch-score was associated with the inactivation of the cell cycle signaling and the activation of the PI3K-AKT-mTOR and VEGF pathways (Figure 4E), corroborated by its correlations with low sensitivities to the agents causing cell-cycle arrest and high sensitivities to the PI3K-AKT-mTOR and VEGFR inhibitors (Figure 4G). These results indicate that the ccRCCs with a high Notch-score might respond well to VEGFR/mTOR inhibitors.

The Notch-score predicts the benefits from avelumab plus axitinib over sunitinib

We further investigated the association of the Notch-score with the benefit from immunotherapy over VEGFR/mTOR inhibitors in two large datasets from the JAVELIN (avelumab plus axitinib vs. sunitinib) and the CM-009/010/025 trials (nivolumab vs. everolimus).

To explore a cutoff value of the Notch-score with optimal predictive power and verify it, the 726 ccRCC patients with available RNA-seq data in the JAVELIN cohort were randomly separated into a training set (n = 484) and a validation set (n = 242) with a ratio of 2:1. The basic characteristics and the Notch-score of this cohort are shown in Figure 5A. The difference in the association of a biomarker with survival across treatment arms is the essential proof of its predictive utility.[36] In the training set, for each cutoff value ranging from 20^{th} to 80^{th} percentiles, we calculated the treatment effect in the below-cutoff and the above-cutoff subgroups. The treatment effect was larger in the low Notch-score group than the high Notch-score group at all cutoffs (Figure 5B). The difference in treatment effect between these two subgroups reached its maximum at the cutoff of the 64.7^{th} percentile (interaction hazard ratio [HR] = 0.47, 95% confidence interval [CI] 0.27–0.80, p = 0.006, Figure 5B). At this cutoff, the benefit from avelumab plus axitinib over sunitinib was considerable in the low Notch-score group (HR = 0.48, 95% CI 0.34–0.67, Log rank p < 0.001) while negligible in the high Notch-score group (HR = 0.99, 95% CI 0.64–1.52, Log rank p = 0.95, Figure 5C). Comparable results were observed in the validation set using the same cutoff (low Notch-score: HR = 0.63, 95% CI 0.40–0.98, Log rank p = 0.039; high Notch-score: HR = 1.01, 95% CI 0.54–1.89, Log rank p = 0.97, Figure 5D).

In the total set of all 726 patients, patients with a low Notch-score had higher survival on avelumab plus axitinib and poorer survival on sunitinib monotherapy, leading to a larger benefit (Figure 5E). The interaction effect between the Notch-score and treatment effect was significant (interaction HR = 0.55, 95% CI 0.35–0.85, p = 0.007, Table S3). We performed a multivariable analysis using the data provided by the JAVELIN researchers involving age, sex, programmed cell death-ligand 1 (PD-L1), $CD8^+$ T cell, tumor mutational burden, intratumoral heterogeneity, and the clusters defined by the TCGA Research Network study.[33] The interaction effect remained significant in the multivariable model (multivariable interaction HR = 0.55, 95% CI 0.35–0.86, p = 0.008, Table S3).

As endogenous NOTCH antagonists, delta-like non-canonical Notch ligand 1/2 (DLK1/2) can bind NOTCH receptors competitively with canonical ligands such as Jagged1 and DLL4, thereby reducing Notch activity.[37] In response to acute renal inflammation, *DLK1* expression was more dramatically modified compared to *DLK2*.[38] In ccRCCs where the Notch pathway is commonly activated,[30] *DLK1* was lowly expressed while *DLK2* had higher expression in comparison to normal kidney tissues.[39,40] These previous findings suggest that within DLK1 and DLK2, DLK1 might function as a major inhibitor of Notch activity in ccRCCs. Given these, we hypothesized that DLK1, rather than DLK2, may possess the opposite predictive power of the Notch-score.

In the JAVELIN cohort, the mRNA data shared by researchers have two significant figures with a minimum scale value of 0.01. 80.9% and 34.8% of samples had expression of *DLK1* and *DLK2* of 0.01, respectively, resulting in poor discrimination in these fractions of samples. Therefore, we sought to analyze the associations of *DLK1/2* expression with treatment benefits in the samples with expression above 0.01. High

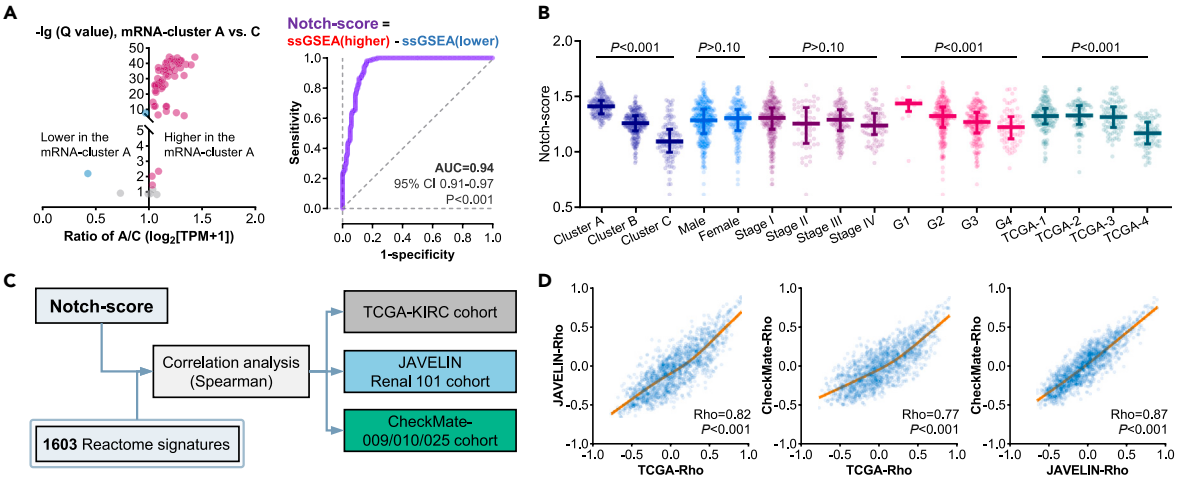

E

Notch signaling	TCGA Rho	TCGA -lg(Q)	JAVELIN Rho	JAVELIN -lg(Q)	CheckMate Rho	CheckMate -lg(Q)
Notch signaling	0.67	64.58	0.26	11.45	0.51	20.10
NOTCH1: ICD regulates transcription	0.76	93.87	0.73	119.41	0.77	57.96
NOTCH1: signal to the nucleus	0.73	84.26	0.58	63.12	0.36	9.46
NOTCH2: ICD regulates transcription	0.82	118.96	0.76	134.27	0.74	52.05
NOTCH2: signal to the nucleus	0.71	77.71	0.53	51.69	0.38	10.77
NOTCH3: ICD regulates transcription	0.74	87.06	0.72	113.50	0.75	55.42
NOTCH3: signal to the nucleus	0.63	55.49	0.49	42.52	0.44	14.19
NOTCH4: ICD regulates transcription	0.75	91.56	0.70	106.62	0.69	41.66
NOTCH4: signal to the nucleus	0.88	164.87	0.88	232.28	0.73	50.87

DNA damage repair	TCGA Rho	TCGA -lg(Q)	JAVELIN Rho	JAVELIN -lg(Q)	CheckMate Rho	CheckMate -lg(Q)
Homologous recombination repair	-0.41	20.94	-0.29	14.13	-0.40	11.77
Mismatch repair	-0.36	15.73	-0.24	10.28	-0.22	3.67
Nucleotide excision repair	-0.27	8.75	-0.46	37.91	-0.37	10.24
Base excision repair	-0.38	17.52	-0.23	9.30	-0.14	1.66
Non-homologous end joining	-0.13	2.22	-0.27	12.58	-0.33	7.89
Fanconi anemia pathway	-0.48	29.46	-0.21	7.71	-0.36	9.36
Translesion synthesis	-0.21	5.51	-0.27	12.89	-0.28	5.79
G1/S DNA damage checkpoint	-0.48	29.32	-0.50	45.09	-0.32	7.43
G2/M DNA damage checkpoint	-0.45	25.61	-0.39	25.67	-0.49	18.20

Cell cycle, PI3K-AKT, and cell death	TCGA Rho	TCGA -lg(Q)	JAVELIN Rho	JAVELIN -lg(Q)	CheckMate Rho	CheckMate -lg(Q)
Cell cycle	-0.25	7.53	-0.35	21.09	-0.38	10.53
Cell cycle mitotic	-0.22	6.08	-0.35	20.89	-0.36	9.26
Mitotic G1 and G1/S transition	-0.30	10.68	-0.42	30.37	-0.38	10.58
Mitotic G2 and M	-0.25	7.89	-0.38	25.24	-0.32	7.58
Cell cycle checkpoints	-0.43	22.86	-0.40	28.52	-0.44	14.50
G2/M checkpoints	-0.52	34.52	-0.45	35.92	-0.45	15.23
Mitotic spindle checkpoints	-0.31	11.94	-0.33	18.58	-0.41	12.50
PI3K-AKT signaling	0.36	16.11	0.20	6.81	0.24	4.41
Apoptosis	0.01	0.06	-0.36	21.86	-0.26	4.89
Necrosis	-0.14	2.52	-0.15	4.34	-0.15	1.77
Pyroptosis	-0.21	5.27	-0.27	12.20	-0.16	2.03
Autophagy	-0.36	15.56	-0.44	34.36	-0.24	4.19

Immune activation and VEGF signaling	TCGA Rho	TCGA -lg(Q)	JAVELIN Rho	JAVELIN -lg(Q)	CheckMate Rho	CheckMate -lg(Q)
Ag processing: ubiquitination proteasome	-0.28	9.44	-0.35	20.52	-0.29	6.22
Ag presentation: MHC-I	-0.34	13.98	-0.30	15.14	-0.27	5.33
Ag presentation: MHC-II	-0.40	19.06	-0.30	15.09	-0.11	1.13
Ag presentation: cross presentation	-0.23	6.50	-0.30	15.69	-0.24	4.45
BCR signaling	-0.12	1.90	-0.22	8.22	-0.27	5.32
TCR signaling	-0.14	2.63	-0.20	7.29	-0.20	3.10
Metabolism of steroids	-0.38	17.22	-0.39	26.44	-0.31	6.79
TGF-beta famiy signaling	0.56	40.99	0.24	9.79	0.34	8.22
VEGF signaling	0.53	36.19	0.46	36.79	0.48	17.20
VEGF/VEGFR interactions	0.82	119.68	0.76	134.51	0.67	38.85
VEGFR2-mediated vascular permeability	0.25	7.64	0.24	10.20	0.46	16.09
VEGFR2-mediated cell proliferation	0.34	13.94	0.23	9.10	0.35	9.06

F Immune cell infiltration (CIBERSORT)

	B Cells Memory	B Cells Naive	Dendritic Cells Activated	Dendritic Cells Resting	Eosinophils	Macrophages M0	Macrophages M1	Macrophages M2	Mast Cells Activated	Mast Cells Resting	Monocytes	Neutrophils	NK Cells Activated	NK Cells Resting	Plasma Cells	T Cells CD4 Memory Activated	T Cells CD4 Memory Resting	T Cells CD4 Naive	T Cells CD8	T Cells Follicular Helper	T Cells gamma delta	T Cells Regulatory
TCGA Rho	-0.12	0.15	0.02	-0.14	-0.14	-0.12	0.05	0.03	-0.04	0.21	0.15	-0.14	-0.07	0.22	0.08	-0.12	0.22	-0.13	-0.11	-0.15	-0.14	-0.17
-lg(Q)	1.93	2.74	0.14	2.48	2.51	2.05	0.58	0.27	0.36	5.20	2.77	2.38	0.86	5.23	1.02	2.04	5.25	2.23	1.71	2.77	2.38	3.09
JAVELIN Rho	0.01	-0.02	0.06	-0.08	-0.09	0.03	-0.10	0.08	-0.12	0.23	0.06	-0.22	-0.10	0.26	-0.01	-0.12	-0.02	0.02	-0.12	-0.04	-0.13	0.13
-lg(Q)	0.07	0.15	0.73	1.30	1.52	0.30	1.63	1.24	2.41	8.20	0.76	7.81	1.66	10.35	0.07	2.43	0.13	0.13	2.49	0.45	2.76	2.76
CheckMate Rho	-0.05	-0.04	0.08	-0.11	-0.17	0.01	-0.18	-0.05	0.13	0.16	0.19	-0.16	-0.10	0.32	0.27	-0.18	0.10	0.09	-0.15	0	-0.25	0.02
-lg(Q)	0.32	0.30	0.72	1.03	2.13	0.07	2.33	0.32	1.30	1.87	2.34	1.87	0.84	6.56	4.87	2.33	0.89	0.80	1.65	0.03	4.33	0.13

Q<0.05 in all three cohorts

G Drug sensitivity (IC_{50})

	HDAC			Cell cycle			PARP			PI3K-AKT-mTOR				VEGFR				
	Vorinostat	Entinostat	RO-3306	Serdemetan	Nutlin-3a	Palbociclib	Olaparib	Rucaparib	Veliparib	AZD6482	GDC0941	MK-2206	AZD8055	Axitinib	Sunitinib	Pazopanib	Sorafenib	Motesanib
Rho	-0.49	-0.32	0.13	0.15	0.20	0.20	-0.47	-0.25	-0.14	-0.25	-0.57	-0.38	-0.36	-0.26	-0.17	-0.39	-0.11	-0.44
-lg(Q)	31.15	12.74	2.50	3.01	5.27	5.43	28.76	7.95	2.71	7.71	43.63	18.26	16.61	8.69	3.97	19.27	1.72	24.62

Figure 4. Construction of the Notch-score and its associations with clinicopathological features, Reactome pathways, and immune cell infiltration

(A) Volcano plot illustrating the differences of the mRNA levels of the Notch pathway genes between the mRNA-clusters A and C; the formula of the Notch score and its utility in differentiating the samples of the mRNA-clusters A and C.

(B) Association between the Notch-score and clinicopathological features. Data are displayed as median and quartiles.

(C) Diagram of the analysis based on the Notch score and Reactome pathways.

(D) The correlation of the Rho values of a single signature between three datasets (TCGA, JAVELIN Renal 101, and CheckMate-009/010/025).

(E and F) Associations of the Notch-score with the ssGSEA scores of 1603 Reactome pathways (E) and immune cell infiltration (F).

(G) Associations of the Notch-score with drug sensitivity in the Genomics of Drug Sensitivity database. Abbreviations: AUC = area under curve, CI = confidence interval, CIBERSORT = Cell-type identification by estimating relative subsets of RNA transcripts, IC_{50} = half-maximal inhibitory concentration levels, TPM = transcripts per kilobase million, ssGSEA = single sample gene set enrichment analysis.

DLK1 expression was linked with a larger benefit at nearly all cutoffs (Figure 5F), while the treatment effects in the high *DLK2* group and the low *DLK2* group were comparable (Figure 5G).

As we observed associations of a high Notch-score with high sensitivity to sunitinib in cell lines (Figure 4G) and long PFS on first-line sunitinib (Figure 5E), we planned to further validate these findings in the E-MTAB-3267 cohort containing 53 ccRCC patients with available mRNA data treated with sunitinib in the first-line setting.[41] A high Notch-score was associated with long PFS at all available cutoffs (Figure 5H). At the cutoff of 64.7th percentile, the HR was 1.55 (95% CI 0.80–3.01) with a Log rank p value of 0.19; the statistical power was limited by the small sample size. In addition, high *DLK1* expression trended to be associated with short PFS with a greater degree compared to *DLK2* (Figure 5I).

Taken together, a high Notch-score was linked with a limited benefit from avelumab plus axitinib over sunitinib, indicating that the ccRCCs with a high Notch-score may not benefit from additional ICI on top of VEGFR tyrosine kinase inhibitor (TKI). The predictive power of the Notch-score was further corroborated by the opposite predictive value of *DLK1* expression.

The Notch-score predicts the benefits from nivolumab over everolimus

In the CM-009/010/025 cohort, we calculated the Notch-score of the 311 patients with available RNA-seq data (Figure 6A). At the cutoff (the 64.7th percentile) derived from the training set of the JAVELIN cohort, the interaction effect was significant (HR = 0.61, 95% CI 0.37–1.00, p = 0.049, Figure 6B). Nivolumab delivered a significant PFS benefit over everolimus in the low Notch-score subgroup (HR = 0.73, 95% CI 0.54–1.00, p = 0.046) rather than in the high Notch-score subgroup (HR = 1.15, 95% CI 0.77–1.70, p = 0.91, Figure 6C). Moreover, the interaction effect remained significant in the multivariable model (multivariable interaction HR = 0.58, 95% CI 0.35–0.96, p = 0.035, Table S3). In addition, high expression of *DLK1*, rather than *DLK2*, was associated with a high treatment benefit (Figures 6D and 6E), consistent with previously described findings in the JAVELIN cohort (Figures 5F and 5G). These findings revealed the relationship between a high Notch-score and a limited benefit from nivolumab over everolimus. In summary, compared to VEGFR/mTOR inhibitors, ICI-based immunotherapies might be recommended for the Notch-activated ccRCCs.

DISCUSSION

In this study, we first observed that most (50/62) Notch pathway genes differentially expressed in ccRCCs compared with normal renal tissues. Based on the mRNA expression of the Notch pathway genes, ccRCC samples were classified into three clusters with different immune characteristics and prognoses. Next, we constructed the Notch-score representing Notch activation and observed the associations of a low Notch-score with the inactivation of the VEGF and the PI3K-AKT-mTOR pathways and inflamed TIME in three independent cohorts. Furthermore, we revealed that a low Notch-score may predict poor sensitivities to VEGFR/mTOR inhibitors in ccRCC cell lines and remarkable benefits from ICI-based immunotherapy to VEGFR/mTOR inhibitors in the JAVELIN and the CM-009/010/025 trials.

Notch activation exerts multiple oncogenic effects, such as CSC maintenance, induction of epithelial-mesenchymal transition, angiogenesis, and inhibition of apoptosis.[42] In ccRCC, inhibition of the Notch signaling blocks the proliferation and self-renewal of CSCs in organoids and impairs tumor growth in patient-derived xenografts in mice.[30,43,44] In our study, the mRNA-cluster A with higher expression of most Notch pathway genes had the longest OS among all clusters. These observations might be seemingly counterintuitive. However, in cell and animal experiments, the difference between experimental and control groups was usually whether activation of the Notch pathway in the same cell line or xenograft (self-contrasted method); in the clinical cohort analysis, it was comparing tumors that were dependent on the Notch pathway to those possibly dependent on other pathways. Different types of ccRCCs may depend on different pathways, and Notch-dependent ccRCCs may progress more slowly than those dependent on other pathways, thus exhibiting a relatively better prognosis. Similar results can also be observed in previously published articles where genomic alterations of Notch pathway genes and high expression of *JAG1/2*, *NOTCH1*, *DLL4*, and *HEY1* are associated with better survival.[29,30] This phenomenon can also be observed in other cancer types. For instance, *EML4-ALK* translocation, a well-known oncogenic genomic alteration in lung adenocarcinoma, was associated with better survival.[45] Based on our findings and published results from other researchers, oncogenic impacts and the association with better prognosis may not be conflicting.

Notch activation can affect the activity of other cancer-related signaling pathways, such as PI3K-AKT, TGF-β, HIF1α,[11] VEGFR1,[22] VEGFR2,[22,46] cell cycle,[47–49] and DNA damage response.[50,51] In the present study, we also observed the associations of the Notch-score with the pathways described previously, indicating that our Notch-score can efficiently reflect Notch activation and these associations might,

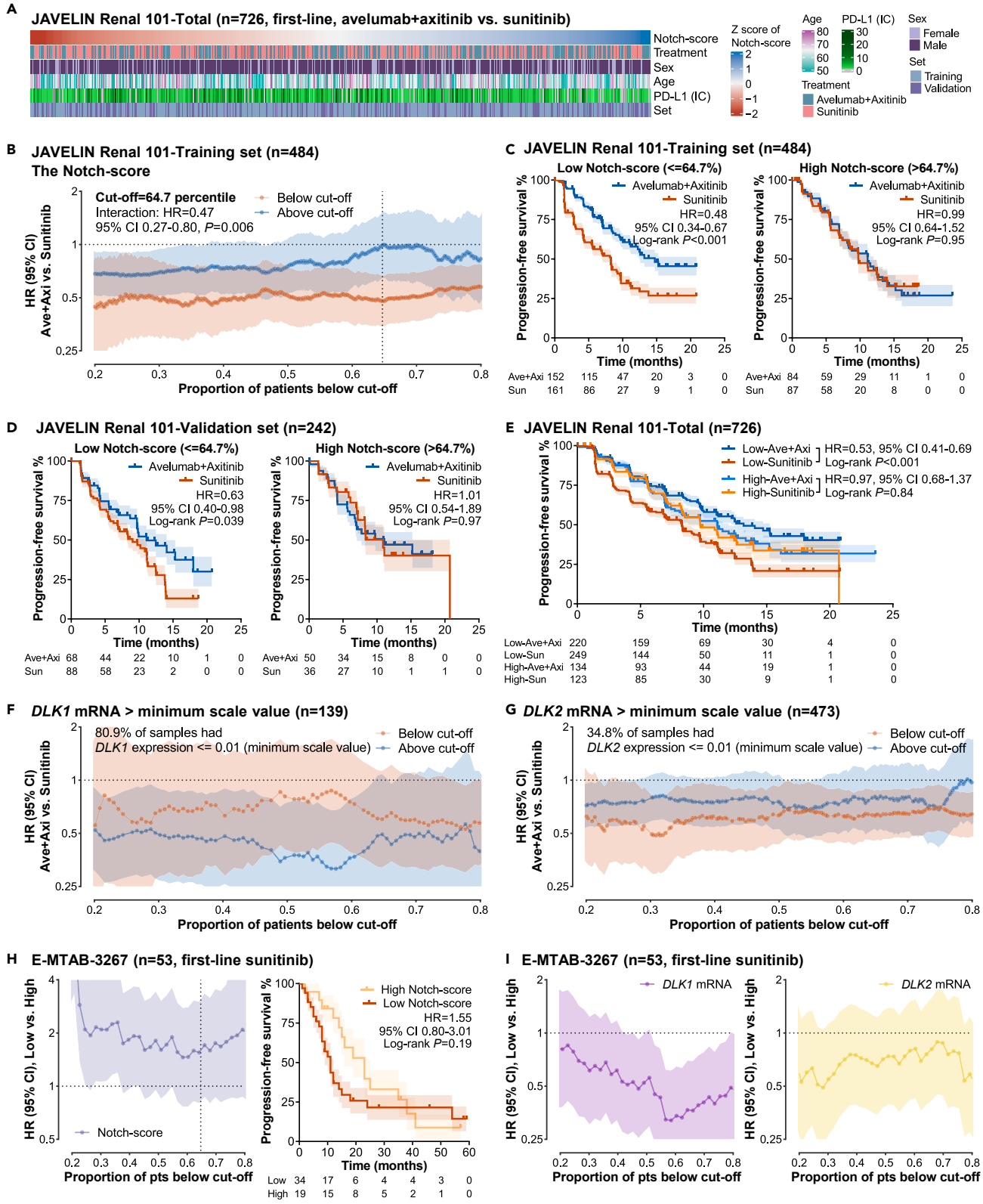
A
JAVELIN Renal 101-Total (n=726, first-line, avelumab+axitinib vs. sunitinib)
Notch-score
Treatment
Sex
Age
PD-L1 (IC)
Set
Z score of Notch-score
Age
PD-L1 (IC)
Sex
Female
Male
Set
Training
Validation
Treatment
Avelumab+Axitinib
Sunitinib
B
JAVELIN Renal 101-Training set (n=484)
The Notch-score
Cut-off=64.7 percentile
Interaction: HR=0.47
95% CI 0.27-0.80, P=0.006
Below cut-off
Above cut-off
HR (95% CI) Ave+Axi vs. Sunitinib
Proportion of patients below cut-off
C
JAVELIN Renal 101-Training set (n=484)
Low Notch-score (<=64.7%)
High Notch-score (>64.7%)
Avelumab+Axitinib
Sunitinib
HR=0.48
95% CI 0.34-0.67
Log-rank P<0.001
HR=0.99
95% CI 0.64-1.52
Log-rank P=0.95
Progression-free survival %
Time (months)
Ave+Axi 152 115 47 20 3 0
Sun 161 86 27 9 1 0
Ave+Axi 84 59 29 11 1 0
Sun 87 58 20 8 0 0
D
JAVELIN Renal 101-Validation set (n=242)
Low Notch-score (<=64.7%)
High Notch-score (>64.7%)
Avelumab+Axitinib
Sunitinib
HR=0.63
95% CI 0.40-0.98
Log-rank P=0.039
HR=1.01
95% CI 0.54-1.89
Log-rank P=0.97
Progression-free survival %
Time (months)
Ave+Axi 68 44 22 10 1 0
Sun 88 58 23 2 0 0
Ave+Axi 50 34 15 8 0 0
Sun 36 27 10 1 1 0
E
JAVELIN Renal 101-Total (n=726)
Low-Ave+Axi
Low-Sunitinib
HR=0.53, 95% CI 0.41-0.69
Log-rank P<0.001
High-Ave+Axi
High-Sunitinib
HR=0.97, 95% CI 0.68-1.37
Log-rank P=0.84
Progression-free survival %
Time (months)
Low-Ave+Axi 220 159 69 30 4 0
Low-Sun 249 144 50 11 1 0
High-Ave+Axi 134 93 44 19 1 0
High-Sun 123 85 30 9 1 0
F
DLK1 mRNA > minimum scale value (n=139)
80.9% of samples had
DLK1 expression <= 0.01 (minimum scale value)
Below cut-off
Above cut-off
HR (95% CI) Ave+Axi vs. Sunitinib
Proportion of patients below cut-off
G
DLK2 mRNA > minimum scale value (n=473)
34.8% of samples had
DLK2 expression <= 0.01 (minimum scale value)
Below cut-off
Above cut-off
HR (95% CI) Ave+Axi vs. Sunitinib
Proportion of patients below cut-off
H
E-MTAB-3267 (n=53, first-line sunitinib)
HR (95% CI), Low vs. High
Notch-score
Proportion of pts below cut-off
High Notch-score
Low Notch-score
HR=1.55
95% CI 0.80-3.01
Log-rank P=0.19
Progression-free survival %
Time (months)
Low 34 17 6 4 4 3 0
High 19 15 8 5 2 1 0
I
E-MTAB-3267 (n=53, first-line sunitinib)
DLK1 mRNA
DLK2 mRNA
HR (95% CI), Low vs. High
Proportion of pts below cut-off

Figure 5. Notch-score as a predictor of the benefit from avelumab plus axitinib over sunitinib

(A) Heatmap illustrating the Notch-score and clinicopathological features of the JAVELIN Renal 101 cohort.

(B) The associations of the cutoff value with the interaction effect between the Notch-score and treatment effect (avelumab plus axitinib vs. sunitinib) and the treatment effect in the above- and the below-cutoff groups in the training set of the JAVELIN Renal 101 cohort.

(C–E) The treatment effect (avelumab plus axitinib vs. sunitinib) in the low and the high Notch-score groups in the training set (C), the validation set (D), and the total set (E) of the JAVELIN Renal 101 cohort.

(F and G) The associations of the cutoff value with the interaction effect between *DLK1* (F) and *DLK2* (G) mRNA expression and treatment effect (avelumab plus axitinib vs. sunitinib) and the treatment effect in the above- and the below-cutoff groups in the JAVELIN Renal 101 cohort.

(H and I) Associations of the PFS on first-line sunitinib with the Notch-score (H) and *DLK1/2* mRNA expression (I). All the shadow area represents the 95% CI.

Abbreviations: CI = confidence interval, HR = hazard ratio, IC = immune cell, PD-L1 = programmed cell death-ligand 1.

at least in part, account for the predictive effect of the Notch-score on the sensitivities to targeted agents, such as the inhibitors of VEGFR, PI3K-AKT-mTOR, PARP, and cell cycle.

In TIME, the NOTCH ligands on myeloid-derived suppressor cells (MDSCs) interact with tumoral NOTCH receptors and thereby improve the CSC capacity,[52] which in turn increases the expression of NOTCH ligands on MDSCs,[21] constituting positive feedback which eventually results in immune tolerance.[27] Treatment with blocking anti-Jagged1/2 had substantial, CD8-dependent therapeutic benefits in several mouse cancer models, possibly underlying the mechanism of inducing the appearance of $CD11c^{+}$, potentially immunostimulatory MDSC-like cells.[21] Here, we also observed that the ccRCCs with a higher Notch-score or in the Notch-activated cluster had more "resting"/"anti-inflammatory" rather than "activated"/"pro-inflammatory" TIICs. In addition, the negative correlations of the Notch-score with antigen processing/presentation and B/T cell receptor downstream signaling also suggest the immune-suppressive tumor microenvironment of the ccRCCs with a high Notch-score.

The difference in the treatment effects in the subgroups identified by the biomarker is the essential proof of its predictive utility.[36] In some previous studies, comparisons were performed within each arm (i.e., compare the survival of the high Notch-score and the low Notch-score subgroups in the immunotherapy arm).[24–26,53] These comparisons can identify biomarkers to estimate the survival of patients undergoing immunotherapy; however, these biomarkers cannot guide the treatment choice. Despite the significant survival benefits from ICI-based immunotherapies over VEGFR/mTOR inhibitors in the intention-to-treat population,[54–60] part of the patients may not acquire these benefits and the high cost of immunotherapy can be saved in this subpopulation. In our study, we compared the survival data of immunotherapy arms and VEGFR/mTOR inhibitor arms in the high Notch-score and the low Notch-score subgroups. Considerable benefits from ICI-based therapies over VEGFR/mTOR inhibitors were observed in the low Notch-score subgroup, while scarcely no benefits were revealed in the high Notch-score group (accounting for 35.3% of patients), identifying the Notch-score as a quantitative predictive biomarker for the benefits from ICI-based immunotherapies over VEGF/mTOR inhibitors. These findings were further confirmed by the antithetical predictive power of *DLK1*, acting as an endogenous antagonist of the Notch pathway in ccRCCs.[40] These results may indicate that ICIs did not provide advantages and might not be strongly recommended for the Notch-activated ccRCCs, by which the cost-effectiveness of antitumor treatments in advanced ccRCCs may be potentially improved.

In patient-derived ccRCC xenografts, blocking the DLL4-NOTCH binding induces an endothelial hyper-sprouting phenotype characterized by excessive production of aberrant non-functional tumor vessels, and the antitumor effect of DLL4 antibodies can be potentiated by VEGF inhibition.[61] Despite the antiangiogenic impact, the DLL4 blockade would have the potential advantage of blocking other effects of DLL4 in CSCs.[42] Bispecific DLL4-VEGF mAbs, navicixizumab and ABL-001 (NOV-1501), are well tolerated and effective against solid tumors.[62,63] Of great interest, whether the dual blockade of DLL4 and VEGF may improve ICI efficacy in the Notch-activated ccRCCs can be preliminarily explored in xenograft mouse models. In our study, Notch-activated ccRCCs had poor immunotherapy benefits, raising a speculation that whether Notch inhibitors could increase immunotherapy efficacy. Previously in triple-negative breast cancer xenograft models, combination of the γ-secretase inhibitor (GSI) inhibiting Notch pathway and anti-PD-1 induced a strikingly larger reduction in the tumor growth rate compared to GSI or anti-PD-1 alone,[64] suggesting that combination of Notch inhibitors and ICIs might potentially sensitize tumors that are otherwise therapy resistant when treated with ICIs alone. Further studies are warranted to investigate whether Notch inhibitors can serve as immunotherapeutic adjuvants to improve ICI efficacy in the Notch-activated ccRCCs.

In the clinical setting, the Notch-score held the promising potential to identify patients that could hardly benefit from ICI-based immunotherapy over VEGFR/mTOR inhibitors in advanced/metastatic ccRCCs. For those with a high Notch-score, sunitinib monotherapy and avelumab plus axitinib led to paralleled survival, indicating that ICIs may not be appropriate for these populations, thereby reducing unnecessary wastage of ICIs and the risks of side effects. In addition, the Notch-score may be used to recognize Notch-activated ccRCC xenografts and organoids, guiding the investigations on whether Notch inhibitors can serve as immunotherapeutic adjuvants to improve immunotherapy efficacy.

To our knowledge, this is the first comprehensive analysis delineating the immune correlates of Notch pathway genes and evaluating their utilities in predicting immunotherapy benefit in ccRCCs. Our findings demonstrate the potential utility of the Notch pathway in guiding treatment choice (immunotherapies vs. VEGFR/mTOR inhibitors) in advanced/metastatic ccRCCs, for the optimization of ICI treatment in clinical practice.

Limitations of the study

As for limitations, first, the Notch-score was constructed as a proxy of actual pathway activation. Despite the strong correlations between the Notch-score and the ssGSEA scores of all NOTCH1-4 pathways in three large datasets, the specific features correlated

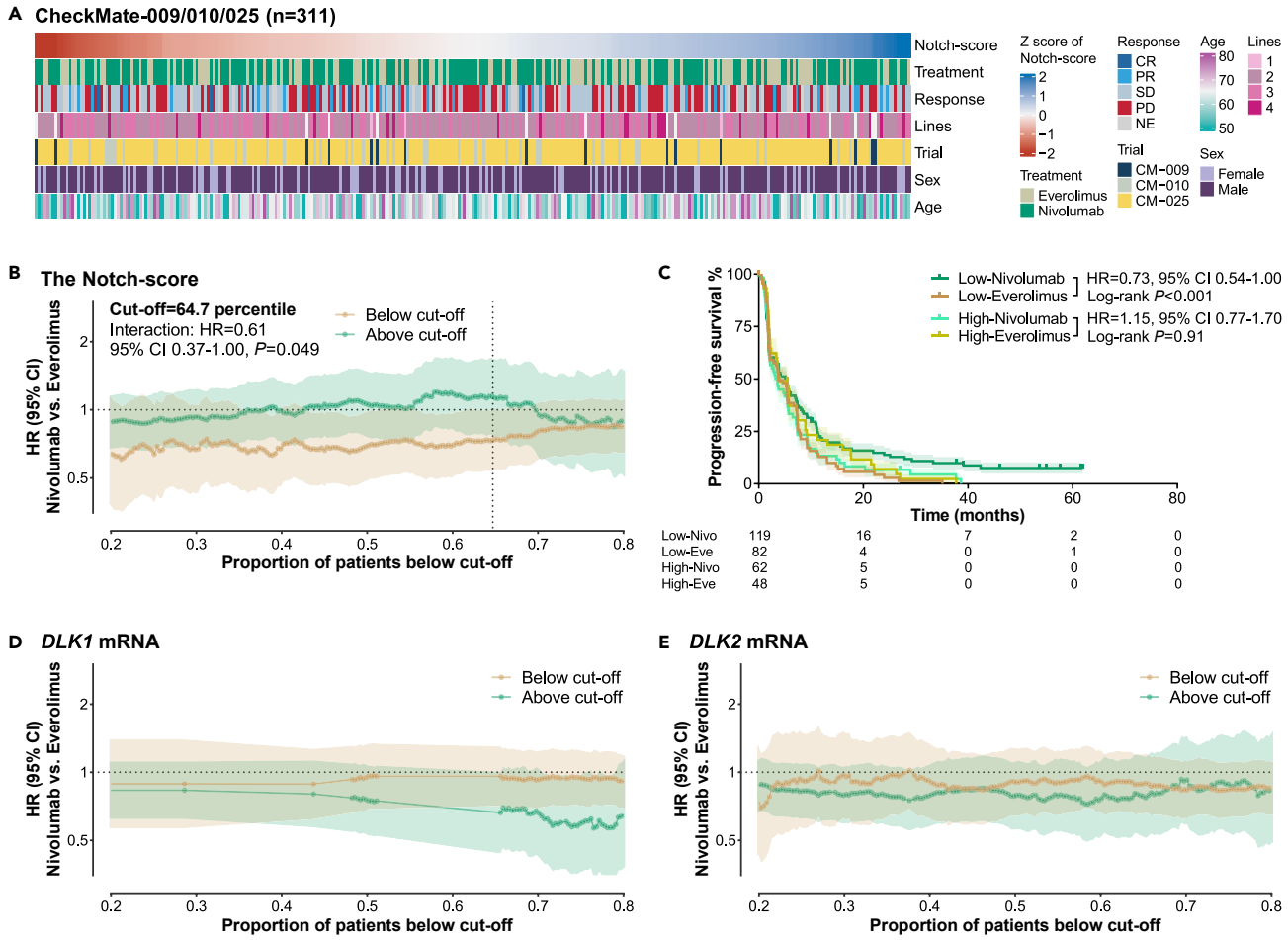

Figure 6. Notch-score as a predictor of the benefit from nivolumab over everolimus

(A) Heatmap illustrating the Notch-score and clinicopathological features of the CM-009/010/025 cohort.

(B) The associations of the cutoff value with the interaction effect between the Notch-score and treatment effect (nivolumab vs. everolimus) and the treatment effect in the above- and the below-cutoff groups of the CM-009/010/025 cohort.

(C) The treatment effect (nivolumab vs. everolimus) in the low and the high Notch-score groups of the CM-009/010/025 cohort.

(D and E) The associations of the cutoff value with the interaction effect between *DLK1* (D) and *DLK2* (E) mRNA expression and treatment effect (nivolumab vs. everolimus) and the treatment effect in the above- and the below-cutoff groups in the CM-009/010/025 cohort. All the shadow area represents the 95% CI.

Abbreviations: CI = confidence interval, CM = CheckMate, CR = complete response, HR = hazard ratio, NE = not evaluable, PD = progressive disease, PD-L1 = programmed cell death-ligand 1, PR = partial response, SD = stable disease.

with the Notch-score might be controlled by the pathways other than Notch. Second, the Notch-score constructed in the TCGA-KIRC dataset dominated by localized ccRCCs might not effectively reflect the features of advanced ccRCCs. However, the associations of the Notch-score with Notch activation, other cancer-related pathways, and immune cell infiltration were parallel between the TCGA-KIRC cohort and the other two large cohorts of advanced/metastatic ccRCCs. These results demonstrate the robustness of the Notch-score in both early-stage and late-stage ccRCCs and also suggest its potential utility in predicting ICI benefits in both neoadjuvant and adjuvant settings. Third, the Notch-score was constructed using the tissue-bulk mRNA data, and thereby whether the Notch activation in tumor cells or stromal/immune cells is associated with immunotherapy benefit cannot be explored in our study. Further studies using single-cell RNA sequencing data are warranted. Fourth, the retrospective setting of our study may introduce biases, which can be minimized by the context of large randomized trials and the implementation of multivariable analysis and independent validation. Fifth, in our study, the ICI regimens analyzed are avelumab plus axitinib and nivolumab monotherapy, which may represent anti-PD-(L)1 plus VEGFR TKI and anti-PD-(L)1 monotherapy, respectively. More data are needed to further validate the robustness of the predictive power of the Notch-score. Unfortunately, due to the lack of patient-level data, it is not available to validate our results in the CheckMate-214 and the IMmotion151 trials in this study.[24,65] In the biomarker analysis of CM-214, more advantages from nivolumab plus ipilimumab over sunitinib were observed in the patients with a high level of tumor-infiltrating neutrophil,[24] which was associated with a low Notch-score in our study. The biomarker

analysis of the IMmotion151 trial revealed the co-occurrence of high expression of NOTCH, TGF-β, and angiogenesis modules in the cluster 1 (angio/stromal) with limited benefit from atezolizumab plus bevacizumab over sunitinib,[65] consistent with our results. Given these, Notch activation might be a robust biomarker predicting poorer benefit from immunotherapies over VEGFR/mTOR inhibitors. Previous studies have elucidated the associations of efficacious immunotherapy with the loss-of-function mutations in NOTCH receptor genes in non-small cell lung cancers[66–68] and colorectal cancers[69] and with Notch activation in small-cell lung cancers.[70] Future research is warranted to explore whether Notch inactivation can predict a larger immunotherapy benefit in other solid tumors. Much more work would be needed to warrant drug development targeting the Notch signaling in ccRCCs using xenograft and organoid model systems where causality can be evaluated.

STAR★METHODS

Detailed methods are provided in the online version of this paper and include the following:

- KEY RESOURCES TABLE
- RESOURCE AVAILABILITY
  - Lead contact
  - Materials availability
  - Data and code availability
- EXPERIMENTAL MODEL AND STUDY PARTICIPANT DETAILS
  - Clinical cohorts
  - Cell lines
- METHOD DETAILS
  - Study design
  - Definition of the Notch pathway genes
  - Construction of the mRNA-lncRNA network
  - Unsupervised clustering based on the mRNA data
  - Calculation of the Notch-score and other pathway scores
  - Cell-type identification by estimating relative subsets of RNA transcripts (CIBERSORT)
- QUANTIFICATION AND STATISTICAL ANALYSIS

SUPPLEMENTAL INFORMATION

Supplemental information can be found online at https://doi.org/10.1016/j.isci.2023.108290.

ACKNOWLEDGMENTS

This work was supported by the CAMS Initiative for Innovative Medicine (2021-I2M-1-015). We thank Dizai Shi (Stitch) for his emotional support and the patients included and their family members for their understanding and participation.

AUTHOR CONTRIBUTIONS

S.H., Y.X., and N.X. designed this study. Y.X. developed methodology. S.H. and Y.X. acquired the data. Y.X. performed analyses. All authors participated in writing, review, and/or revision of the manuscript. G.W., S.C., and N.X. provided administrative, technical, or material support. N.X. supervised this study.

DECLARATION OF INTERESTS

Y.X., Q.Z., G.W., L.L., and S.C. are employees of Burning Rock Biotech.

INCLUSION AND DIVERSITY

We worked to ensure diversity in experimental samples through the selection of the cell lines. We worked to ensure diversity in experimental samples through the selection of the genomic datasets. One or more of the authors of this paper self-identifies as a member of the LGBTQIA+ community. We avoided "helicopter science" practices by including the participating local contributors from the region where we conducted the research as authors on the paper.

Received: March 15, 2023
Revised: August 29, 2023
Accepted: October 18, 2023
Published: October 21, 2023

REFERENCES

1. Sung, H., Ferlay, J., Siegel, R.L., Laversanne, M., Soerjomataram, I., Jemal, A., and Bray, F. (2021). Global cancer statistics 2020: GLOBOCAN estimates of incidence and mortality worldwide for 36 cancers in 185 countries. CA. Cancer J. Clin. *71*, 209–249. https://doi.org/10.3322/caac.21660.
2. Jonasch, E., Walker, C.L., and Rathmell, W.K. (2021). Clear cell renal cell carcinoma ontogeny and mechanisms of lethality. Nat. Rev. Nephrol. *17*, 245–261. https://doi.org/10.1038/s41581-020-00359-2.
3. Jonasch, E., Gao, J., and Rathmell, W.K. (2014). Renal cell carcinoma. BMJ *349*, g4797. https://doi.org/10.1136/bmj.g4797.
4. Hsieh, J.J., Purdue, M.P., Signoretti, S., Swanton, C., Albiges, L., Schmidinger, M., Heng, D.Y., Larkin, J., and Ficarra, V. (2017). Renal cell carcinoma. Nat. Rev. Dis. Primers *3*, 17009. https://doi.org/10.1038/nrdp.2017.9.
5. Brodziak, A., Sobczuk, P., Bartnik, E., Fiedorowicz, M., Porta, C., Szczylik, C., and Czarnecka, A.M. (2019). Drug resistance in papillary RCC: from putative mechanisms to clinical practicalities. Nat. Rev. Urol. *16*, 655–673. https://doi.org/10.1038/s41585-019-0233-z.
6. Bi, K., He, M.X., Bakouny, Z., Kanodia, A., Napolitano, S., Wu, J., Grimaldi, G., Braun, D.A., Cuoco, M.S., Mayorga, A., et al. (2021). Tumor and immune reprogramming during immunotherapy in advanced renal cell carcinoma. Cancer Cell *39*, 649–661.e5. https://doi.org/10.1016/j.ccell.2021.02.015.
7. Derosa, L., Routy, B., Fidelle, M., Iebba, V., Alla, L., Pasolli, E., Segata, N., Desnoyer, A., Pietrantonio, F., Ferrere, G., et al. (2020). Gut Bacteria Composition Drives Primary Resistance to Cancer Immunotherapy in Renal Cell Carcinoma Patients. Eur. Urol. *78*, 195–206. https://doi.org/10.1016/j.eururo.2020.04.044.
8. Radtke, F., MacDonald, H.R., and Tacchini-Cottier, F. (2013). Regulation of innate and adaptive immunity by Notch. Nat. Rev. Immunol. *13*, 427–437. https://doi.org/10.1038/nri3445.
9. Zhang, S., Miyakawa, A., Wickström, M., Dyberg, C., Louhivuori, L., Varas-Godoy, M., Kemppainen, K., Kanatani, S., Kaczynska, D., Ellström, I.D., et al. (2022). GIT1 protects against breast cancer growth through negative regulation of Notch. Nat. Commun. *13*, 1537. https://doi.org/10.1038/s41467-022-28631-y.
10. Jeffries, S., and Capobianco, A.J. (2000). Neoplastic transformation by Notch requires nuclear localization. Mol. Cell Biol. *20*, 3928–3941. https://doi.org/10.1128/mcb.20.11.3928-3941.2000.
11. Ayaz, F., and Osborne, B.A. (2014). Non-canonical notch signaling in cancer and immunity. Front. Oncol. *4*, 345. https://doi.org/10.3389/fonc.2014.00345.
12. Mukherjee, M., Fogarty, E., Janga, M., and Surendran, K. (2019). Notch Signaling in Kidney Development, Maintenance, and Disease. Biomolecules *9*, 692. https://doi.org/10.3390/biom9110692.
13. Jeong, H.W., Jeon, U.S., Koo, B.K., Kim, W.Y., Im, S.K., Shin, J., Cho, Y., Kim, J., and Kong, Y.Y. (2009). Inactivation of Notch signaling in the renal collecting duct causes nephrogenic diabetes insipidus in mice. J. Clin. Invest. *119*, 3290–3300. https://doi.org/10.1172/jci38416.
14. Niranjan, T., Bielesz, B., Gruenwald, A., Ponda, M.P., Kopp, J.B., Thomas, D.B., and Susztak, K. (2008). The Notch pathway in podocytes plays a role in the development of glomerular disease. Nat. Med. *14*, 290–298. https://doi.org/10.1038/nm1731.
15. Siebel, C., and Lendahl, U. (2017). Notch Signaling in Development, Tissue Homeostasis, and Disease. Physiol. Rev. *97*, 1235–1294. https://doi.org/10.1152/physrev.00005.2017.
16. Li, Z., Xin, S., Yu, S., Liang, J., and Zhang, X. (2022). Prognostic Signatures and Therapeutic Value Based on the Notch Pathway in Renal Clear Cell Carcinoma. Oxid. Med. Cell. Longev. *2022*, 1669664. https://doi.org/10.1155/2022/1669664.
17. Lasagni, L., Ballerini, L., Angelotti, M.L., Parente, E., Sagrinati, C., Mazzinghi, B., Peired, A., Ronconi, E., Becherucci, F., Bani, D., et al. (2010). Notch activation differentially regulates renal progenitors proliferation and differentiation toward the podocyte lineage in glomerular disorders. Stem Cells (Dayton, Ohio) *28*, 1674–1685. https://doi.org/10.1002/stem.492.
18. Takebe, N., Miele, L., Harris, P.J., Jeong, W., Bando, H., Kahn, M., Yang, S.X., and Ivy, S.P. (2015). Targeting Notch, Hedgehog, and Wnt pathways in cancer stem cells: clinical update. Nat. Rev. Clin. Oncol. *12*, 445–464. https://doi.org/10.1038/nrclinonc.2015.61.
19. Bayik, D., and Lathia, J.D. (2021). Cancer stem cell-immune cell crosstalk in tumour progression. Nat. Rev. Cancer *21*, 526–536. https://doi.org/10.1038/s41568-021-00366-w.
20. Shen, Q., Cohen, B., Zheng, W., Rahbar, R., Martin, B., Murakami, K., Lamorte, S., Thompson, P., Berman, H., Zúñiga-Pflücker, J.C., et al. (2017). Notch Shapes the Innate Immunophenotype in Breast Cancer. Cancer Discov. *7*, 1320–1335. https://doi.org/10.1158/2159-8290.CD-17-0037.
21. Sierra, R.A., Trillo-Tinoco, J., Mohamed, E., Yu, L., Achyut, B.R., Arbab, A., Bradford, J.W., Osborne, B.A., Miele, L., and Rodriguez, P.C. (2017). Anti-Jagged Immunotherapy Inhibits MDSCs and Overcomes Tumor-Induced Tolerance. Cancer Res. *77*, 5628–5638. https://doi.org/10.1158/0008-5472.CAN-17-0357.
22. Kangsamaksin, T., Murtomaki, A., Kofler, N.M., Cuervo, H., Chaudhri, R.A., Tattersall, I.W., Rosenstiel, P.E., Shawber, C.J., and Kitajewski, J. (2015). NOTCH decoys that selectively block DLL/NOTCH or JAG/NOTCH disrupt angiogenesis by unique mechanisms to inhibit tumor growth. Cancer Discov. *5*, 182–197. https://doi.org/10.1158/2159-8290.CD-14-0650.
23. Vano, Y.A., Elaidi, R., Bennamoun, M., Chevreau, C., Borchiellini, D., Pannier, D., Maillet, D., Gross-Goupil, M., Tournigand, C., Laguerre, B., et al. (2022). Nivolumab, nivolumab-ipilimumab, and VEGFR-tyrosine kinase inhibitors as first-line treatment for metastatic clear-cell renal cell carcinoma (BIONIKK): a biomarker-driven, open-label, non-comparative, randomised, phase 2 trial. Lancet Oncol. *23*, 612–624. https://doi.org/10.1016/S1470-2045(22)00128-0.
24. Motzer, R.J., Choueiri, T.K., McDermott, D.F., Powles, T., Vano, Y.A., Gupta, S., Yao, J., Han, C., Ammar, R., Papillon-Cavanagh, S., et al. (2022). Biomarker analysis from CheckMate 214: nivolumab plus ipilimumab versus sunitinib in renal cell carcinoma. J. Immunother. Cancer *10*, e004316. https://doi.org/10.1136/jitc-2021-004316.
25. Motzer, R.J., Robbins, P.B., Powles, T., Albiges, L., Haanen, J.B., Larkin, J., Mu, X.J., Ching, K.A., Uemura, M., Pal, S.K., et al. (2020). Avelumab plus axitinib versus sunitinib in advanced renal cell carcinoma: biomarker analysis of the phase 3 JAVELIN Renal 101 trial. Nat. Med. *26*, 1733–1741. https://doi.org/10.1038/s41591-020-1044-8.
26. McDermott, D.F., Huseni, M.A., Atkins, M.B., Motzer, R.J., Rini, B.I., Escudier, B., Fong, L., Joseph, R.W., Pal, S.K., Reeves, J.A., et al. (2018). Clinical activity and molecular correlates of response to atezolizumab alone or in combination with bevacizumab versus sunitinib in renal cell carcinoma. Nat. Med. *24*, 749–757. https://doi.org/10.1038/s41591-018-0053-3.
27. Janghorban, M., Xin, L., Rosen, J.M., and Zhang, X.H.F. (2018). Notch Signaling as a Regulator of the Tumor Immune Response: To Target or Not To Target? Front. Immunol. *9*, 1649. https://doi.org/10.3389/fimmu.2018.01649.
28. Majidinia, M., Alizadeh, E., Yousefi, B., Akbarzadeh, M., and Zarghami, N. (2016). Downregulation of Notch Signaling Pathway as an Effective Chemosensitizer for Cancer Treatment. Drug Res. *66*, 571–579. https://doi.org/10.1055/s-0042-111821.
29. Feng, C., Xiong, Z., Jiang, H., Ding, Q., Fang, Z., and Hui, W. (2016). Genetic alteration in notch pathway is associated with better prognosis in renal cell carcinoma. Biofactors *42*, 41–48. https://doi.org/10.1002/biof.1250.
30. Bhagat, T.D., Zou, Y., Huang, S., Park, J., Palmer, M.B., Hu, C., Li, W., Shenoy, N., Giricz, O., Choudhary, G., et al. (2017). Notch Pathway Is Activated via Genetic and Epigenetic Alterations and Is a Therapeutic Target in Clear Cell Renal Cancer. J. Biol. Chem. *292*, 837–846. https://doi.org/10.1074/jbc.M116.745208.
31. Mariathasan, S., Turley, S.J., Nickles, D., Castiglioni, A., Yuen, K., Wang, Y., Kadel, E.E., III, Koeppen, H., Astarita, J.L., Cubas, R., et al. (2018). TGFbeta attenuates tumour response to PD-L1 blockade by contributing to exclusion of T cells. Nature *554*, 544–548. https://doi.org/10.1038/nature25501.
32. Lee, S.M., Jeong, Y.H., Kim, H.M., Park, H.Y., Yoon, D., Kim, D.H., Saeki, S., Moon, S.J., and Kang, M.J. (2009). Presenilin enhancer-2 (PSENEN), a component of the gamma-secretase complex, is involved in adipocyte differentiation. Domest. Anim. Endocrinol. *37*, 170–180. https://doi.org/10.1016/j.domaniend.2009.05.003.
33. Cancer Genome Atlas Research Network (2013). Comprehensive molecular characterization of clear cell renal cell carcinoma. Nature *499*, 43–49. https://doi.org/10.1038/nature12222.
34. Silva, F., Félix, A., and Serpa, J. (2016). Functional redundancy of the Notch pathway in ovarian cancer cell lines. Oncol. Lett. *12*, 2686–2691. https://doi.org/10.3892/ol.2016.4959.
35. Poulaki, V., Mitsiades, C.S., Kotoula, V., Negri, J., McMullan, C., Miller, J.W., Marks, P.A., and Mitsiades, N. (2009). Molecular sequelae of histone deacetylase inhibition in human retinoblastoma cell lines: clinical implications. Invest. Ophthalmol. Vis. Sci. *50*, 4072–4079. https://doi.org/10.1167/iovs.09-3517.

36. Ballman, K.V. (2015). Biomarker: Predictive or Prognostic? J. Clin. Oncol. *33*, 3968–3971. https://doi.org/10.1200/JCO.2015.63.3651.
37. Sánchez-Solana, B., Nueda, M.L., Ruvira, M.D., Ruiz-Hidalgo, M.J., Monsalve, E.M., Rivero, S., García-Ramírez, J.J., Díaz-Guerra, M.J.M., Baladrón, V., and Laborda, J. (2011). The EGF-like proteins DLK1 and DLK2 function as inhibitory non-canonical ligands of NOTCH1 receptor that modulate each other's activities. Biochim. Biophys. Acta *1813*, 1153–1164. https://doi.org/10.1016/j.bbamcr.2011.03.004.
38. Weidenbusch, M., Rodler, S., Song, S., Romoli, S., Marschner, J.A., Kraft, F., Holderied, A., Kumar, S., Mulay, S.R., Honarpisheh, M., et al. (2017). Gene expression profiling of the Notch-AhR-IL22 axis at homeostasis and in response to tissue injury. Biosci. Rep. *37*, BSR20170099. https://doi.org/10.1042/BSR20170099.
39. Lee, M.G., Lee, Y.K., Huang, S.C., Chang, C.L., Ko, C.Y., Lee, W.C., Chen, T.Y., Tzou, S.J., Huang, C.Y., Tai, M.H., et al. (2022). DLK2 Acts as a Potential Prognostic Biomarker for Clear Cell Renal Cell Carcinoma Based on Bioinformatics Analysis. Genes *13*, 629. https://doi.org/10.3390/genes13040629.
40. Kawakami, T., Chano, T., Minami, K., Okabe, H., Okada, Y., and Okamoto, K. (2006). Imprinted DLK1 is a putative tumor suppressor gene and inactivated by epimutation at the region upstream of GTL2 in human renal cell carcinoma. Hum. Mol. Genet. *15*, 821–830. https://doi.org/10.1093/hmg/ddl001.
41. Beuselinck, B., Job, S., Becht, E., Karadimou, A., Verkarre, V., Couchy, G., Giraldo, N., Rioux-Leclercq, N., Molinié, V., Sibony, M., et al. (2015). Molecular subtypes of clear cell renal cell carcinoma are associated with sunitinib response in the metastatic setting. Clin. Cancer Res. *21*, 1329–1339. https://doi.org/10.1158/1078-0432.CCR-14-1128.
42. Majumder, S., Crabtree, J.S., Golde, T.E., Minter, L.M., Osborne, B.A., and Miele, L. (2021). Targeting Notch in oncology: the path forward. Nat. Rev. Drug Discov. *20*, 125–144. https://doi.org/10.1038/s41573-020-00091-3.
43. Fendler, A., Bauer, D., Busch, J., Jung, K., Wulf-Goldenberg, A., Kunz, S., Song, K., Myszczyszyn, A., Elezkurtaj, S., Erguen, B., et al. (2020). Inhibiting WNT and NOTCH in renal cancer stem cells and the implications for human patients. Nat. Commun. *11*, 929. https://doi.org/10.1038/s41467-020-14700-7.
44. Sjölund, J., Johansson, M., Manna, S., Norin, C., Pietras, A., Beckman, S., Nilsson, E., Ljungberg, B., and Axelson, H. (2008). Suppression of renal cell carcinoma growth by inhibition of Notch signaling *in vitro* and *in vivo*. J. Clin. Invest. *118*, 217–228. https://doi.org/10.1172/JCI32086.
45. Wu, S.G., Kuo, Y.W., Chang, Y.L., Shih, J.Y., Chen, Y.H., Tsai, M.F., Yu, C.J., Yang, C.H., and Yang, P.C. (2012). EML4-ALK translocation predicts better outcome in lung adenocarcinoma patients with wild-type EGFR. J. Thorac. Oncol. *7*, 98–104. https://doi.org/10.1097/JTO.0b013e3182370e30.
46. Yan, H., Zhu, L., Zhang, J., and Lin, Z. (2021). Histone demethylase KDM4D inhibition suppresses renal cancer progression and angiogenesis through JAG1 signaling. Cell Death Discov. *7*, 284. https://doi.org/10.1038/s41420-021-00682-y.
47. Khan, F., Singh, V.K., Saeed, M., Kausar, M.A., and Ansari, I.A. (2019). Carvacrol Induced Program Cell Death and Cell Cycle Arrest in Androgen-Independent Human Prostate Cancer Cells via Inhibition of Notch Signaling. Anti Cancer Agents Med. Chem. *19*, 1588–1608. https://doi.org/10.2174/1871520619666190731152942.
48. Sriuranpong, V., Borges, M.W., Ravi, R.K., Arnold, D.R., Nelkin, B.D., Baylin, S.B., and Ball, D.W. (2001). Notch signaling induces cell cycle arrest in small cell lung cancer cells. Cancer Res. *61*, 3200–3205.
49. Jia, Y., Lin, R., Jin, H., Si, L., Jian, W., Yu, Q., and Yang, S. (2019). MicroRNA-34 suppresses proliferation of human ovarian cancer cells by triggering autophagy and apoptosis and inhibits cell invasion by targeting Notch 1. Biochimie *160*, 193–199. https://doi.org/10.1016/j.biochi.2019.03.011.
50. Adamowicz, M., Vermezovic, J., and d'Adda di Fagagna, F. (2016). NOTCH1 Inhibits Activation of ATM by Impairing the Formation of an ATM-FOXO3a-KAT5/Tip60 Complex. Cell Rep. *16*, 2068–2076. https://doi.org/10.1016/j.celrep.2016.07.038.
51. Vermezovic, J., Adamowicz, M., Santarpia, L., Rustighi, A., Forcato, M., Lucano, C., Massimiliano, L., Costanzo, V., Bicciato, S., Del Sal, G., and d'Adda di Fagagna, F. (2015). Notch is a direct negative regulator of the DNA-damage response. Nat. Struct. Mol. Biol. *22*, 417–424. https://doi.org/10.1038/nsmb.3013.
52. Welte, T., Kim, I.S., Tian, L., Gao, X., Wang, H., Li, J., Holdman, X.B., Herschkowitz, J.I., Pond, A., Xie, G., et al. (2016). Oncogenic mTOR signalling recruits myeloid-derived suppressor cells to promote tumour initiation. Nat. Cell Biol. *18*, 632–644. https://doi.org/10.1038/ncb3355.
53. Braun, D.A., Hou, Y., Bakouny, Z., Ficial, M., Sant' Angelo, M., Forman, J., Ross-Macdonald, P., Berger, A.C., Jegede, O.A., Elagina, L., et al. (2020). Interplay of somatic alterations and immune infiltration modulates response to PD-1 blockade in advanced clear cell renal cell carcinoma. Nat. Med. *26*, 909–918. https://doi.org/10.1038/s41591-020-0839-y.
54. Motzer, R.J., Tannir, N.M., McDermott, D.F., Arén Frontera, O., Melichar, B., Choueiri, T.K., Plimack, E.R., Barthélémy, P., Porta, C., George, S., et al. (2018). Nivolumab plus Ipilimumab versus Sunitinib in Advanced Renal-Cell Carcinoma. N. Engl. J. Med. *378*, 1277–1290. https://doi.org/10.1056/NEJMoa1712126.
55. Motzer, R.J., Escudier, B., McDermott, D.F., George, S., Hammers, H.J., Srinivas, S., Tykodi, S.S., Sosman, J.A., Procopio, G., Plimack, E.R., et al. (2015). Nivolumab versus Everolimus in Advanced Renal-Cell Carcinoma. N. Engl. J. Med. *373*, 1803–1813. https://doi.org/10.1056/NEJMoa1510665.
56. Choueiri, T.K., Powles, T., Burotto, M., Escudier, B., Bourlon, M.T., Zurawski, B., Oyervides Juárez, V.M., Hsieh, J.J., Basso, U., Shah, A.Y., et al. (2021). Nivolumab plus Cabozantinib versus Sunitinib for Advanced Renal-Cell Carcinoma. N. Engl. J. Med. *384*, 829–841. https://doi.org/10.1056/NEJMoa2026982.
57. Rini, B.I., Plimack, E.R., Stus, V., Gafanov, R., Hawkins, R., Nosov, D., Pouliot, F., Alekseev, B., Soulières, D., Melichar, B., et al. (2019). Pembrolizumab plus Axitinib versus Sunitinib for Advanced Renal-Cell Carcinoma. N. Engl. J. Med. *380*, 1116–1127. https://doi.org/10.1056/NEJMoa1816714.
58. Motzer, R., Alekseev, B., Rha, S.Y., Porta, C., Eto, M., Powles, T., Grünwald, V., Hutson, T.E., Kopyltsov, E., Méndez-Vidal, M.J., et al. (2021). Lenvatinib plus Pembrolizumab or Everolimus for Advanced Renal Cell Carcinoma. N. Engl. J. Med. *384*, 1289–1300. https://doi.org/10.1056/NEJMoa2035716.
59. Rini, B.I., Powles, T., Atkins, M.B., Escudier, B., McDermott, D.F., Suarez, C., Bracarda, S., Stadler, W.M., Donskov, F., Lee, J.L., et al. (2019). Atezolizumab plus bevacizumab versus sunitinib in patients with previously untreated metastatic renal cell carcinoma (IMmotion151): a multicentre, open-label, phase 3, randomised controlled trial. Lancet *393*, 2404–2415. https://doi.org/10.1016/S0140-6736(19)30723-8.
60. Motzer, R.J., Penkov, K., Haanen, J., Rini, B., Albiges, L., Campbell, M.T., Venugopal, B., Kollmannsberger, C., Negrier, S., Uemura, M., et al. (2019). Avelumab plus Axitinib versus Sunitinib for Advanced Renal-Cell Carcinoma. N. Engl. J. Med. *380*, 1103–1115. https://doi.org/10.1056/NEJMoa1816047.
61. Miles, K.M., Seshadri, M., Ciamporcero, E., Adelaiye, R., Gillard, B., Sotomayor, P., Attwood, K., Shen, L., Conroy, D., Kuhnert, F., et al. (2014). Dll4 blockade potentiates the anti-tumor effects of VEGF inhibition in renal cell carcinoma patient-derived xenografts. PLoS One *9*, e112371. https://doi.org/10.1371/journal.pone.0112371.
62. Fu, S., Corr, B.R., Culm-Merdek, K., Mockbee, C., Youssoufian, H., Stagg, R., Naumann, R.W., Wenham, R.M., Rosengarten, R.D., Benjamin, L., et al. (2022). Phase Ib Study of Navicixizumab Plus Paclitaxel in Patients With Platinum-Resistant Ovarian, Primary Peritoneal, or Fallopian Tube Cancer. J. Clin. Oncol. *40*, 2568–2577. https://doi.org/10.1200/JCO.21.01801.
63. Lee, J., Kim, S., Hong, J., Park, Y., Park, J., Kang, W., Lee, K.-W., Kim, J.W., Kim, J.-W., Kim, S.H., et al. (2021). Abstract P02-03: Phase Ia/Ib dose-escalation study of ABL001 (CTX-009, bispecific antibody targeting DLL4 and VEGF-A) as a single agent in patients with advanced solid tumors. Mol. Cancer Ther. *20*, P02-03. https://doi.org/10.1158/1535-7163.Targ-21-p02-03.
64. Meng, J., Jiang, Y.Z., Zhao, S., Tao, Y., Zhang, T., Wang, X., Zhang, Y., Sun, K., Yuan, M., Chen, J., et al. (2022). Tumor-derived Jagged1 promotes cancer progression through immune evasion. Cell Rep. *38*, 110492. https://doi.org/10.1016/j.celrep.2022.110492.
65. Motzer, R.J., Banchereau, R., Hamidi, H., Powles, T., McDermott, D., Atkins, M.B., Escudier, B., Liu, L.F., Leng, N., Abbas, A.R., et al. (2020). Molecular Subsets in Renal Cancer Determine Outcome to Checkpoint and Angiogenesis Blockade. Cancer Cell *38*, 803–817.e4. https://doi.org/10.1016/j.ccell.2020.10.011.
66. Zhang, K., Hong, X., Song, Z., Xu, Y., Li, C., Wang, G., Zhang, Y., Zhao, X., Zhao, Z., Zhao, J., et al. (2020). Identification of deleterious NOTCH mutation as novel predictor to efficacious immunotherapy in NSCLC. Clin. Cancer Res. *26*, 3649–3661. https://doi.org/10.1158/1078-0432.CCR-19-3976.
67. Zhang, F., Wang, J., Xu, Y., Cai, S., Li, T., Wang, G., Li, C., Zhao, L., and Hu, Y. (2022). Co-occurring genomic alterations and immunotherapy efficacy in NSCLC. NPJ Precis. Oncol. *6*, 4. https://doi.org/10.1038/s41698-021-00243-7.
68. Li, X., Wang, Y., Li, X., Feng, G., Hu, S., and Bai, Y. (2021). The Impact of NOTCH Pathway Alteration on Tumor Microenvironment and

Clinical Survival of Immune Checkpoint Inhibitors in NSCLC. Front. Immunol. *12*, 638763. https://doi.org/10.3389/fimmu.2021.638763.

69. Wang, F., Huang, C., Long, J., Zhao, Z.B., Ma, H.Q., Yao, X.Q., Li, L., and Lian, Z.X. (2022). Notch signaling mutations increase intratumor chemokine expression and predict response to immunotherapy in colorectal cancer. BMC Cancer *22*, 933. https://doi.org/10.1186/s12885-022-10032-5.
70. Roper, N., Velez, M.J., Chiappori, A., Kim, Y.S., Wei, J.S., Sindiri, S., Takahashi, N., Mulford, D., Kumar, S., Ylaya, K., et al. (2021). Notch signaling and efficacy of PD-1/PD-L1 blockade in relapsed small cell lung cancer. Nat. Commun. *12*, 3880. https://doi.org/10.1038/s41467-021-24164-y.
71. Shannon, P., Markiel, A., Ozier, O., Baliga, N.S., Wang, J.T., Ramage, D., Amin, N., Schwikowski, B., and Ideker, T. (2003). Cytoscape: a software environment for integrated models of biomolecular interaction networks. Genome Res. *13*, 2498–2504. https://doi.org/10.1101/gr.1239303.
72. Barbie, D.A., Tamayo, P., Boehm, J.S., Kim, S.Y., Moody, S.E., Dunn, I.F., Schinzel, A.C., Sandy, P., Meylan, E., Scholl, C., et al. (2009). Systematic RNA interference reveals that oncogenic KRAS-driven cancers require TBK1. Nature *462*, 108–112. https://doi.org/10.1038/nature08460.
73. Subramanian, A., Tamayo, P., Mootha, V.K., Mukherjee, S., Ebert, B.L., Gillette, M.A., Paulovich, A., Pomeroy, S.L., Golub, T.R., Lander, E.S., and Mesirov, J.P. (2005). Gene set enrichment analysis: a knowledge-based approach for interpreting genome-wide expression profiles. Proc. Natl. Acad. Sci. USA *102*, 15545–15550. https://doi.org/10.1073/pnas.0506580102.
74. Newman, A.M., Liu, C.L., Green, M.R., Gentles, A.J., Feng, W., Xu, Y., Hoang, C.D., Diehn, M., and Alizadeh, A.A. (2015). Robust enumeration of cell subsets from tissue expression profiles. Nat. Methods *12*, 453–457. https://doi.org/10.1038/nmeth.3337.

STAR★METHODS

KEY RESOURCES TABLE

REAGENT or RESOURCE	SOURCE	IDENTIFIER
Deposited data		
Genomics of Drug Sensitivity in Cancer	https://www.cancerrxgene.org/	N/A
The Cancer Genome Atlas-Kidney Renal Clear Cell Carcinoma	https://www.cbioportal.org/	N/A
The JAVELIN Renal 101 trial	Motzer et al., 2020b	N/A
The E-MTAB-3267 cohort	Beuselinck et al.[41]	E-MTAB-3267
The CheckMate-009/010/025 trials	Braun et al.[53]	N/A
Software and algorithms		
ConsensusClusterPlus (CCP)	http://bioconductor.org/packages/ConsensusClusterPlus/	N/A
Cytoscape	http://www.cytoscape.org/	N/A
ssGSEA	http://software.broadinstitute.org/gsea/	N/A
CIBERSORT	https://cibersort.stanford.edu/index.php	N/A
R 4.1.3	https://www.rstudio.com/products/rstudio/download/	N/A

RESOURCE AVAILABILITY

Lead contact

Further information should be directed to and will be fulfilled by the lead contact, Nianzeng Xing (xingnz@cicams.ac.cn).

Materials availability

This study did not generate new unique reagents and cell lines. All resources reported in this paper will be shared by Nianzeng Xing (xingnz@cicams.ac.cn) upon reasonable requests for non-commercial purposes.

Data and code availability

- The authors declare that relevant data supporting the findings of this study are available within the paper and its Supplementary files. The analyzed data of clinical cohorts and cell lines in the present study were downloaded from public databases or published articles. The sources of these data are described in the key resources table.
- In the present study, we did not generate novel algorithm. The code for analyzing data are disclosed in the figshare (https://doi.org/10.6084/m9.figshare.24187416).
- Any additional information is available from the lead contact upon reasonable requests for non-commercial purposes.

EXPERIMENTAL MODEL AND STUDY PARTICIPANT DETAILS

Clinical cohorts

This study analyzed the clinical, genomic, and transcriptomic data of 4 clinical cohorts, including The Cancer Genome Atlas-Kidney Renal Clear Cell Carcinoma (TCGA-KIRC, n = 522), the JAVELIN Renal 101 trial (phase III, avelumab+axitinib vs. sunitinib, n = 726),[25] the E-MTAB-3267 cohort (n = 53),[41] and the CheckMate-009/010/025 trials (CM-009: phase I, nivolumab; CM-010: phase II, nivolumab; CM-025: phase III, nivolumab vs. everolimus; n = 311).[53] The basic features of these cohorts, including sample sizes, outcomes, clinical settings, the platforms of RNA-seq and immunohistochemical (IHC) staining of programmed cell death-ligand 1 (PD-L1), and treatment, are displayed in Table S4.

The detailed methods of trial design and IHC/RNA-seq testing of the analyzed trials are described in ClinicalTrials.gov and the original manuscripts.[25,41,53,55,60] The level of transcriptomic data was measured by $\log_2$(transcripts per kilobase million [TPM]+1) in the present study.

Cell lines

This study analyzed the pharmacogenomic data of ccRCC cell lines acquired from the Genomics of Drug Sensitivity in Cancer (GDSC) database. The basic features are shown in Table S4.

METHOD DETAILS

Study design

In total, there are five parts in our study (Figure 1), including (i) genomic and transcriptomic features of the Notch pathway genes, (ii) prognostic, biological, and immune correlates of the Notch pathway genes, (iii) construction of the Notch-score, (iv) biological and immune correlates of the Notch-score, and (v) implications of the Notch-score in predicting drug sensitivity and benefit from immunotherapy over VEGFR/mTOR inhibitors. The first three parts were implemented in the TCGA-KIRC cohort. After the construction of the Notch-score, its correlations with biological and immune characteristics were explored in three large cohorts (TCGA-KIRC, JAVELIN, and CM-009/010/025) to prove their robustness. In the last part, the linkage between the Notch-score and drug sensitivity was analyzed using the half-maximal inhibitory concentration levels (IC_{50}) and mRNA data of the GDSC database. The associations of the Notch-score with the benefit from immunotherapy over VEGFR/mTOR inhibitors were explored in the JAVELIN, the E-MTAB-3267, and the CM-009/010/025 cohorts.

Since all clinical data analyzed in the present study were acquired from public databases or published articles, approval by committees and informed consents from subjects were waived. This report follows the Strengthening the Reporting of Observational Studies in Epidemiology (STROBE) and the REporting recommendations for tumour MARKer prognostic studies (REMARK) reporting guidelines.

Definition of the Notch pathway genes

Based on the Notch pathway-related signatures in the CbioPortal platform and molecular signatures database (including HALLMARK_NOTCH_SIGNALING, PID_NOTCH_PATHWAY, KEGG_NOTCH_SIGNALING_PATHWAY, REACTOME_SIGNALING_BY_NOTCH, and WP_NOTCH_SIGNALING) and previous researches,[15,27,28] 62 genes (4 Notch receptors, 30 related to transmitting signal to the nucleus, and 28 related to the transcriptional regulation by the NICD, Table S2) were determined as the Notch pathway genes and were analyzed in our study.

Construction of the mRNA-lncRNA network

We analyzed the correlation between each lncRNA and the mRNA expression of each Notch pathway gene. The mRNA-lncRNA pairs with a correlation R value over 0.80 and a P value below 0.05 were selected for constructing the mRNA-lncRNA network, which were further visualized by Cytoscape.[71]

Unsupervised clustering based on the mRNA data

Unsupervised clustering of the TCGA samples based on the mRNA levels of the 62 Notch pathway genes were performed using the Partitioning Around Medoids (PAM) method. The optimal number of clusters was determined based on the curve of the cost change of K-medoids.

Calculation of the Notch-score and other pathway scores

Differentially expressed Notch pathway genes were identified by comparing the mRNA levels of the 62 Notch pathway genes between the cluster with the best prognosis and the cluster with the worst prognosis. Here, we first separately calculated the two single sample gene set enrichment analysis (ssGSEA) scores of the "highly expressed" and the "lowly expressed" genes, and then the value of the ssGSEA score for "highly expressed" genes minus the score for "lowly expressed" genes was defined as the Notch-score.[72,73] The Notch-scores of the analyzed samples were exhibited in the Data S2.

Based on the transcriptomic data of the JAVELIN, the CM-009/010/025, and the TCGA-KIRC cohorts, ssGSEA was introduced to estimate the enrichment scores of 1,603 Reactome and 50 HALLMARK signatures (https://www.gsea-msigdb.org/gsea/msigdb/genesets.jsp).

Cell-type identification by estimating relative subsets of RNA transcripts (CIBERSORT)

CIBERSORT, an online method (https://cibersort.stanford.edu/index.php) for characterizing cell composition of complex tissues from their gene expression profiles,[74] was applied to the enumeration of hematopoietic subsets in mRNA mixtures from TCGA database. CIBERSORT outperformed other methods with respect to noise, unknown mixture content, and closely related cell types.[74]

QUANTIFICATION AND STATISTICAL ANALYSIS

To assess the between-group difference, we used (i) the Fisher exact test for categorical variables, (ii) the Mann-Whitney and the Kruskal-Wallis test for continuous variables, and (iii) the Kaplan-Meier (KM) curves, the Log-rank test, and the Cox proportional-hazards regression model (hazard ratio [HR] and 95% confidence interval [CI]) for time-to-event variables. The variables with a p-value below 0.10 in the univariable cox regression were included in the following multivariable cox regression. Spearman correlation was used to test the correlations between continuous variables. The association between the Notch-score and the mRNA clusters was estimated by the area under the curve (AUC) of receiver operator characteristic (ROC) curve.

All statistical analyses mentioned above were performed using IBM SPSS Statistics 22 or R 4.1.3. The nominal level of significance was set as 5%, and all 95% CIs were 2-sided unless otherwise specified. Adjusted P value (Q value) was calculated using the Benjamini-Hochberg method. All the statistical details can be found in figures and/or figure legends.